Shear-Thinning Hydrogels Derived from Vitamin B5 Analogous Methacrylamide (B5AMA)

By

Krystof Wigmore

A thesis submitted to the
Department of Chemistry
in partial fulfillment of the requirements for the
degree of Bachelor of Science (Honours) in
Chemistry

This thesis has been accepted by:

_____

Dean of Science

Supervisor: Dr. Marya Ahmed

The Department of Chemistry
University of Prince Edward Island
Charlottetown, Prince Edward Island

Table of Contents

List of Figures ..... *iv*

List of Tables ..... *vi*

List of Appendices ..... *vii*

List of Abbreviations ..... *viii*

Acknowledgments ..... *x*

Abstract ..... *xii*

1 Introduction *1*

1.1 Vitamin B5 ..... **1**

1.2 Vitamin B5 Analogues **2**

1.3 Vitamin B5 Analogous Methacrylamide **4**

1.4 Polymers **5**

1.5 Free Radical Polymerization (FRP) **7**

1.6 Hydrogels **9**

1.6.1 Shear-thinning Hydrogels 12

1.6 Project Description **13**

1.6.1 Objectives 13

1.6.2 Description of Objectives 13

2 Experimental *15*

2.1 Materials **15**

2.2 Synthesis of B5AMA **15**

2.2.1 Small Batch Method 15

2.2.2 Big Batch Method 16

2.3 Synthesis of hydrogels **17**

2.3.1 Ultrasonic bath Method 19

2.3.2 Freeze-Thaw Method 22

2.4 Characterization methods **23**

2.4.1 Swelling Kinetics Sample Preparation 23

2.4.2 Dynamic Light Scattering (DLS) Sample Preparation 23

2.4.3 Absorbance Studies 24

2.4.4 Zeta-Potential Sample Preparation 24

3. Results and Discussion *25*

3.1 Synthesis of B5AMA **25**

3.2 Synthesis of Hydrogels with EGDMA and Diallyl Disulfide Crosslinkers **26**

3.2.1 Characterization 26
3.3 Synthesis of Hydrogels with OXAS Crosslinker 29
3.3.1 Characterization 30
5. Future Work 40
6. References 41
7. Appendices 44
Appendix A: NMR Spectra for B5AMA Synthesis (All NMR is taken by collogue Diego Combita) 44
Appendix B: Data and Graphs for Swelling Kinetics 49
Appendix C: Data and Graphs for Dynamic Light Scattering 55
Appendix D: Data for Absorbance Studies 62
Appendix E: Data and Graphs for Zeta-Potential 63

List of Figures

Figure 1.1: Chemical structure of pantothenic acid (Vitamin B5). 1
Figure 1.2: A) pentoyl moiety for which substituents can be added; B) some substituents that can be added to make a vitamin B5 analogues. 3
Figure 1.3: Structure of D-panthenol. 3
Figure 1.4: Scheme of synthesis of B5AMA. 4
Figure 1.5: Monomer and a polymer.[16] 5
Figure 1.6: Different types of polymers[17] 6
Figure 1.7: Shapes of polymers 7
Figure 1.8: Scheme for FRP. R• represents a free radical capable of initiating propagation; M represents a monomer. R_m• and R_n• represents a propagating radical chain with a degree of polymerization of m and n respectively. AB is a chain transfer agent; Pn + Pm represent terminated macromolecules.[14] 8
Figure 1.9: Schematic illustration of the transition behavior of LCST thermo-responsive polymers; the red line represents the macroscopic phase transition. This shows the behavior of an LCST polymer, such as poly(N-isopropylacrylamide) in water. 10
Figure 1.10: Classification of hydrogels.[22] 11
Figure 1.11: Shear-thinning hydrogels and their applications.[27] 12
Figure 2.1: Reaction scheme for B5AMA. 16
Figure 2.2: Column being ran for a big batch of monomer B5AMA. 17
Figure 2.3:Scheme for synthesis of hydrogels. 17
Figure 2.4: Chemical structure and names of all molecules used in the synthesis of hydrogels in this project. 18
Figure 2.5: Hydrogels placed in syringes after ultrasonic bath for use in swelling kinetics. 21
Figure 3.1: Hydrogels after ultrasonic bath method showing white precipitate. 27
Figure 3.2: Hydrogels KW-11-1 and KW-11-2 after ultrasonic bath and gelation. 28
Figure 3.3: Graph for average of swelling kinetics experiments 1, 2, and 3. 29
Figure 3.0.4: Graph of DLS data for KW-7-1 31
Figure 3.5: Graph of DLS data for KW-21-2 31
Figure 3.6: Graph of DLS data for KW-21-1 32
Figure 3.7: Graphs of absorbance data for KW-7-1 (6% OXAS) and KW-7-2 (4% OXAS) 34
Figure 3.8: Graphs of absorbance data for KW-21-1 (10% OXAS) and KW-21-2 (8% OXAS). 35
Figure 7.1:NMR spectrum for KW-5-1. 44
Figure 7.2: NMR spectrum for KW-11. 44
Figure 7.3: NMR spectrum for KW-26. 45
Figure 7.4:NMR spectrum for KW-32. 45
Figure 7.5: NMR spectrum for KW-33. 46
Figure 7.6: NMR spectrum for KW-36. 46
Figure 7.7:NMR spectrum for KW-40. 47
Figure 7.8: NMR spectrum for KW-43. 47
Figure 7.9: NMR spectrum for KW-45. 48
Figure 7.10: Swelling kinetics for KW-10-1. 49
Figure 7.11: Graph for KW-10-2 Swelling Kinetics. 50

Figure 7.12: Graph showing swelling kinetics of KW-13-1 experiment 1. 51
Figure 7.13: Graph showing swelling kinetics of KW-13-1 experiment 2. 52
Figure 7.14: Graph showing swelling kinetics of KW-15-1 experiment 2. 53
Figure 7.15: Graph of DLS data for KW-27-1 with error bars representing standard deviation. 55
Figure 7.16: Graph of DLS data for KW-27-2 with error bars representing standard deviation. 56
Figure 7.17: Graph of DLS data for KW-34-2 with error bars representing standard deviation. 57
Figure 7.18: Graph of DLS data for DFC-722-2 with error bars representing standard deviation. 58
Figure 7.19: Graph of DLS data for KW-7-2..... 61

List of Tables

Table 2.1: Compositions of hydrogels synthesized using the ultrasonic degasification method. * Everything after these were made with filtered DEGMEM and EGDMA 19
Table 2.2: Composition of hydrogel synthesized using ultrasonic degasification method 19
Table 2.3: Compositions of all hydrogels synthesized using the freeze-thaw 22
Table 3.1: All synthesis of B5AMA performed with % Yield. *NMR spectra can be found in appendix A 25
Table 3.2: Reconstituted concentrations 26
Table 3.3: Data for zeta-potential of KW-28-2 37
Table 7.1: Data for swelling kinetics study for KW-10-1 49
Table 7.2: Data for swelling kinetics study for KW-10-2 50
Table 7.3: Data for first swelling kinetics experiment with KW-13-1 51
Table 7.4: Data for second swelling kinetics experiment with KW-13-1 52
Table 7.5: Data for third swelling kinetics experiment with KW-15-1 53
Table 7.6: Data for average of swelling kinetic experiments 1,2 and 3 54
Table 7.7: DLS data for KW-27-1 55
Table 7.8: DLS data for KW-27-2 56
Table 7.9: Data for DLS of KW-34-2 57
Table 7.10: DLS data for DFC-722-2 58
Table 7.11: DLS data for KW-7-1 59
Table 7.12: *DLS data for KW-21-2* 59
Table 7.13: DLS data for KW-21-1 60
Table 7.14: DLS data for KW-7-2 61
Table 7.15: Absorbance data for KW-7 62
Table 7.16: Absorbance data for KW-21 62
Table 7.17: Data for zeta-potential of KW-34-2 63
Table 7.18: Data for zeta-potential of KW-27-1 64
Table 7.19: Data for zeta-potential of KW-37-1 65
Table 7.20: Data for zeta-potential of DFC-722-2 66
Table 7.21: Data for zeta-potential of KW-27-2 67

List of Appendices

Appendix A: NMR Spectra for B5AMA Synthesis (All NMR is taken by collogue Diego Combita)

Appendix B: Data and Graphs for Swelling Kinetics

Appendix C: Data and Graphs for Dynamic Light Scattering

Appendix D: Data for Absorbance Studies

Appendix E: Data and Graphs for Zeta-Potential

List of Abbreviations

ACP: Acyl carrier protein

ACVA: 4,4′-Azobis(4-cyanovaleric acid)

AEMA: 2-aminoethylmethacrylamide hydrochloride

ATRP: Atom transfer radical polymerization

B5AMA: Vitamin B5 Analogous Methacrylamide

CoA: Coenzyme-A

DEGMEM: Di(ethylene glycol) methyl ether methacrylate

DLS: dynamic light scattering

EGDMA: Ethylene glycol dimethacrylate

FRP: Free radical polymerization

KPS: Potassium Persulfate

LCST: Lower concentration solution temperature

LRP: living/controlled radical polymerization

MeOH: Methanol

MW: Molecular weight

NMP: Nitroxide mediated polymerization

OXAS: (3,9-Divinyl-2,4,8,10-tetraoxaspiro[5.5]undecane)

PDI: Polydispersity index

RAFT: Reversible-addition fragmentation chain transfer polymerization TEA: triethylamine

TEMEDA: N,N,N’,N’-tetramethylethylenediamine

TMSPA: Trimethylsilylpropanoic acid

TLC: Thin Layer Chromatography

W_o: Weight of dry hydrogel

W_t: Weight of wet hydrogel

Acknowledgments

It is with immense gratitude that I acknowledge the individuals who have made this research project possible. Their unwavering support and assistance have been invaluable in the successful completion of this project. Firstly, I would like to express my sincerest appreciation to Diego Combita, for his unwavering guidance, patience, and knowledge-sharing throughout this research project. His expertise in the field of chemistry has been instrumental in shaping the direction and outcome of this study. I would also like to thank Stephan Scully, Patricia Boland and Jill MacDonald of the chemistry department for their invaluable assistance in the experimental work. Their dedication and professionalism in providing a conducive environment for the project are much appreciated. I am grateful to all my colleagues, Nauman Nazeer, Adnan Bhayo, Alexandra Pippy, Catherine Doyle, Marinda Steeves, Vineet Kumar Mishra, Samin Jahan, Ranga Dissanayake, Sarah Collins, Vidya Singh, Peggy Doughan, my colleagues' insightful discussions and constructive feedback have contributed immensely to the development of this research. Their collaborations and camaraderie have made the research process all the more enjoyable and fruitful. I would like to express my appreciation to my family and friends for their unwavering support, encouragement, and love throughout this research project. Their emotional support has been invaluable in keeping me motivated and focused throughout the challenging phases of this project. Lastly, I would like to thank my supervisor Dr. Mayra Ahmed for her continued support throughout this project as well as her expertise in the field of chemistry and for giving me the opportunity to conduct this research. Her expertise in the field showed with every question asked, every group meeting attended, and every roadblock that we passed along the way. In conclusion, I am grateful to everyone who has contributed to the success of this research project. Their support,

expertise, and assistance have been invaluable, and I look forward to continuing this journey of discovery with their continued support and encouragement.

Abstract

Hydrogels are a three-dimensional network of synthetic or natural polymers that can take on vast amounts of water. Shear-thinning hydrogels are a specialized type of hydrogels that can be injected by shear stress which causes the hydrogel to flow and will self-heal after shear is removed. Shear thinning hydrogels have been studied for many different applications, including drug delivery, tissue engineering, and cryopreservation of cells, due to their benefits, which include biocompatibility and easy modification. This research focuses on the synthesis and characterization of shear-thinning hydrogels based on Vitamin B5 Analogous Methacrylamide (B5AMA). The synthesis of shear thinning hydrogels is carried out with different comonomer and crosslinker compositions, using free radical polymerization approach. The hydrogels are characterized for their swelling kinetics, dynamic light scattering, zeta-potential, lower critical solution temperature (LCST) determination and rheological behaviour. These materials are then studied for the applications in cryopreservation.

1 Introduction

1.1 Vitamin B5

Vitamin B5 chemically known as pantothenic acid, is one of the eight B vitamins that help the body to convert carbohydrates into glucose.[1] Pantothenic acid is water soluble and is well known for its hygroscopic, antibacterial, biocompatible, and moisturizing activities.[2] Pantothenic acid has been shown to have biological importance in cell growth, fatty acid synthesis, carbohydrate metabolism, amino acid catabolism, and heme synthesis.[2] It is also required to form coenzyme- A (CoA) and acyl carrier, which makes it critical for the metabolism and synthesis of carbohydrates, proteins, and fats.[3] The name pantothenic is derived from the Greek word pantothen, which means "from everywhere," as small amounts of pantothenic acid are found in almost all food.[3] The pantothenic acid structure comprises two moieties, a pantoic acid moiety and a b-alanine moiety. An amide bond joins the two moieties together, and this structure can be seen in **Figure 1.1.**

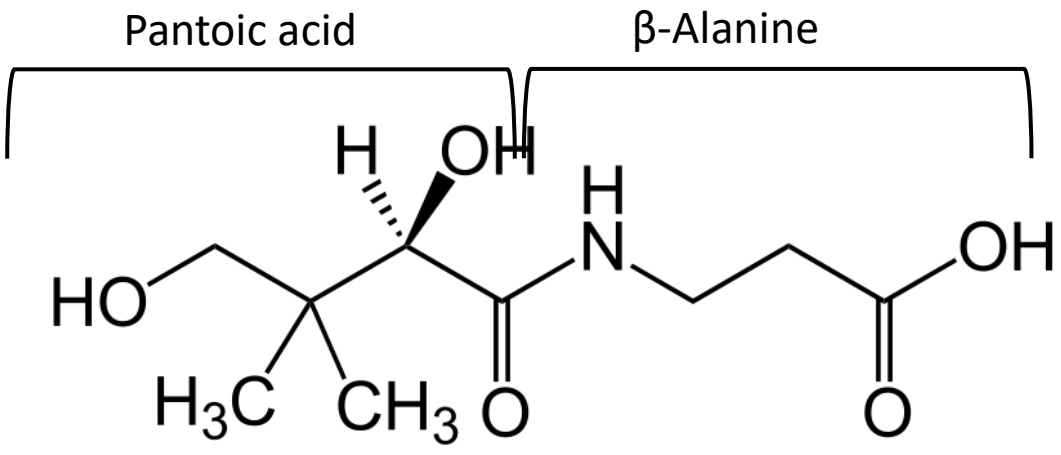

Figure 1.1: Chemical structure of pantothenic acid (Vitamin B5).

Pantothenic acid, found in most foods, exists in the form of CoA or Acyl Carrier Protein (ACP). However, for the vitamin to be absorbed by intestinal cells, it needs to be converted into free pantothenic acid. This conversion occurs in the intestine lumen, where CoA and ACP are broken down into 4'-phosphopantetheine, which is then converted into pantetheine by removing the phosphate group.[3] Pantetheine is further processed by the intestinal enzyme, pantetheinase, to produce free pantothenic acid.[3]

1.2 Vitamin B5 Analogues

Analogues are compounds of a material that have closely similar molecular structure to that of another by replacing one or more atoms with a different atom or functional group. The replacement of β-alanine in the structure of pantothenic acid with a similarly polymerizable methacrylamide moiety can yield pantothenic acid analogues with interesting properties.[2] There have been many vitamin B5 analogues that have been published in the literature, most of which kept the pantoyl moiety and varied by the substituent that was attached to the amide nitrogen.[4] Substituents attached include: alcohols, amides, alkenes, and etc. The uses of these analogues which are shown in **Figure 1.2** were all in a bacteria study to inhibit plasmodium falciparum.[4] Across the literature multiple vitamin B5 analogs have shown antimicrobial activities as such in the paper mentioned above where 8 out of the 10 analogues tested inhibited the proliferation of the plasmodium falciparum.[4] Vitamin B5 analogous are also reported to show antibacterial and antifouling efficacies.[2]

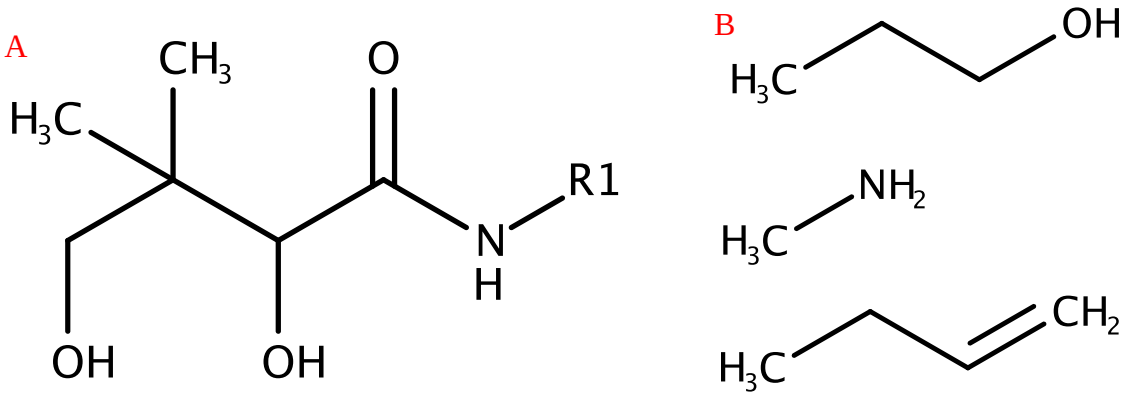

Figure 1.2: A) pentoyl moiety for which substituents can be added; B) some substituents that can be added to make a vitamin B5 analogues.

Some other common analogues of pantothenic acid are panthenol, pantetheine, and pantethine.[5] Panthenol is an alcohol related to pantothenic acid and possess vitamin activity as well. It is readily oxidized to form pantothenic acid in organisms.[5] D-panthenol is the only biologically active species and its chemical structure is shown in **Figure 1.3.**

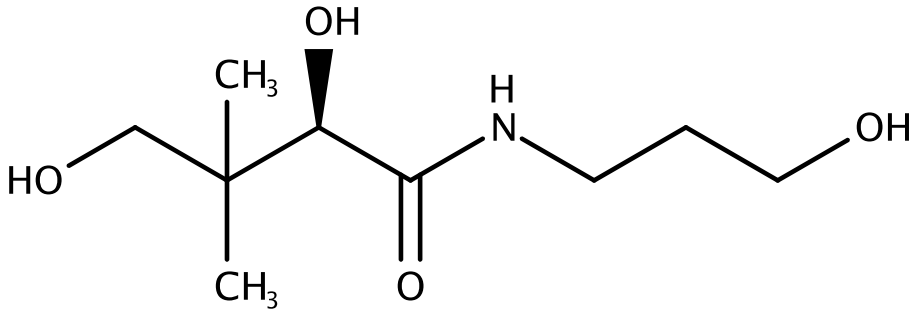

Figure 1.3: Structure of D-panthenol.

This analogue is commonly used in pharmaceutical and cosmetic preparations as it is a hygroscopic viscous oil and can be crystallized.[5] It is used in the cosmetics as a moisturizer as it

is a humectant, so it is ideal for keeping water in the skin and it also helps to protect the skin from environmental factors and stresses.

1.3 Vitamin B5 Analogous Methacrylamide

Vitamin B5 Analogous Methacrylamide (B5AMA) is the vitamin B5 analogue that is used for all the experiments in this thesis. It was first synthesized in 2018 at the University of Prince Edward Island in the Ahmed research group. In that paper they reported a successful synthesis of vitamin B5AMA which was used to produce hygroscopic hydrogels. The monomer B5AMA was synthesized by ring opening chemistry. The synthesis uses 2-aminoethyl methacrylamide (AEMA) and D-pantolactone, where AEMA is synthesized by a previously established procedure.[21] The synthesis scheme is shown in Figure 1.4.

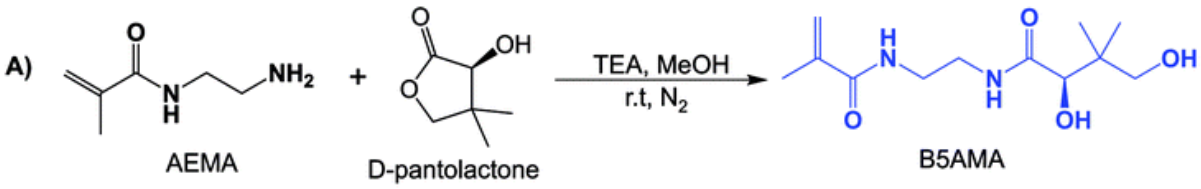

Figure 1.4: Scheme of synthesis of B5AMA.

The hydrogels synthesized using the monomer B5AMA were found to be capable of carrying large amounts of water and were able to absorb and desorb the water repeatably at ambient temperature.[2] They were also found to be salt responsive as well in a paper put out by the Ahmed research lab.[20] In another paper from the Ahmed research group, Combita, *et al*. synthesized poly(B5AMA) coated glass slides and compared their antifouling properties with PEGylated glass slides and the results showed that antifouling properties of poly(B5AMA) are comparable with PEG.[6]

1.4 Polymers

Polymers are long chain molecules which are made up of smaller molecules called monomers as shown in **Figure 1.5**. There are two main types of polymers, natural and synthetic. Natural polymers are found in everyday examples such as lignin or chitosan which are found in wood and crustation shells, respectively. Synthetic polymers on the other hand are synthesized which allows for very good reproducibility as well as control over physical and chemical properties.[24] Some examples of synthetic polymers are plastics and Kevlar.

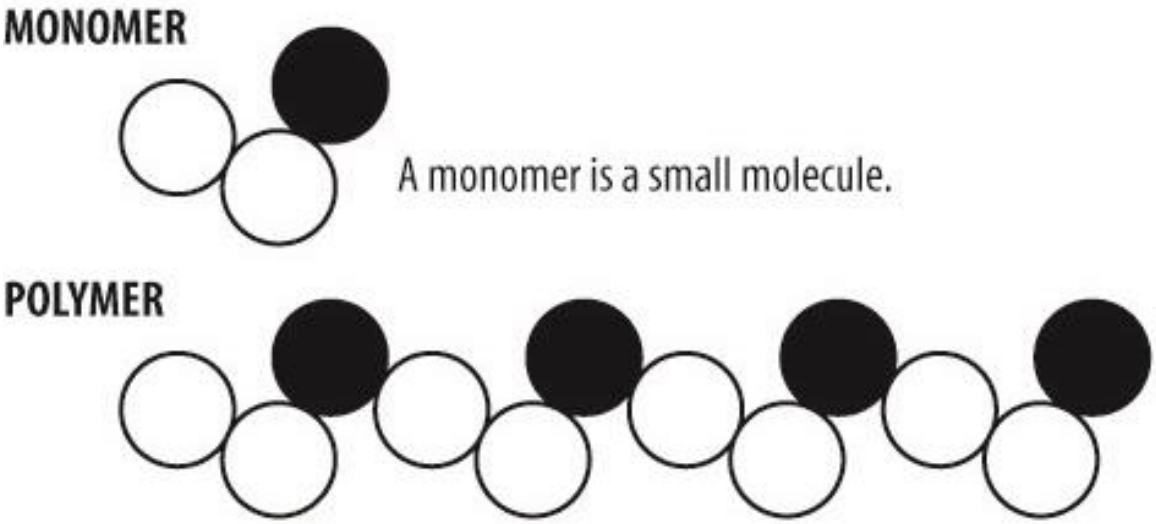

Figure 1.5: Monomer and a polymer.[16]

The classification of polymers is based on many different factors, including source (synthetic or natural), method of synthesis and applications, and composition. According to composition, two main types of polymers are homopolymers which are polymers made up of one single monomer unit while the other is copolymers which can be made of 2 or more monomer subunits.[25] Copolymers can be broken down into even more classes such as random, block, alternating and graft copolymers.[25] Shown in **Figure 1.6** is an example of each.

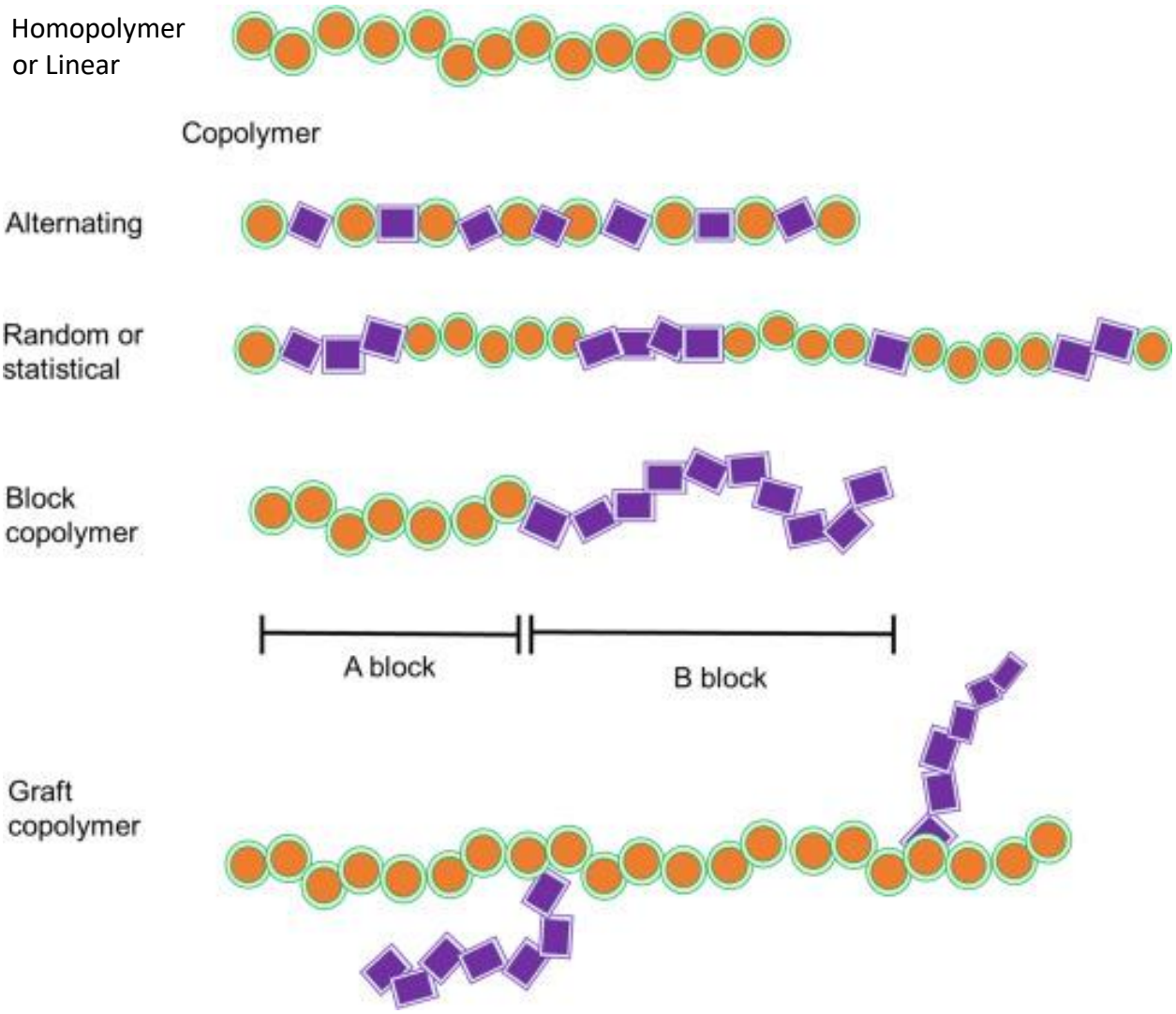

Figure 1.6: Different types of polymers[17]

One of the biggest factors to the chemical and physical properties of polymers are their shape as shown in **Figure 1.7**. Polymers can be linear which is a molecule that has repeating units in a single chain with no branching or they can be branched which is when branches come off the linear backbone of the polymer or they can be crosslinked polymers which are linear polymers that are joined by a branching connection. Crosslinked polymers can also be called network polymers.[25]

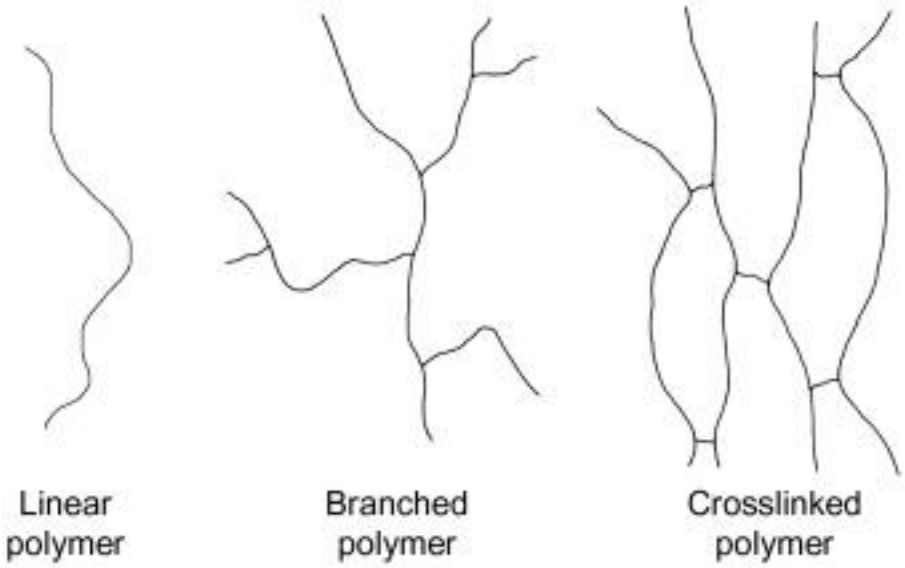

Figure 1.7: Shapes of polymers

Linear polymers are held together by weak van der Waals forces or hydrogen bonding, this makes them easy to break down with stimuli such as heat.[7] Branched polymers can also be easily broken down by heat as the addition of branches does not make the polymer stronger while crosslinked polymers are strongly bonded together with covalent bonding.[25] Crosslinking of polymers can be achieved with a wide variety of different crosslinkers which effect the physical properties of the polymeric materials.[8] The crosslinking of polymers gives a more rigid structure through the chemical linkages.[8] Some examples of crosslinked polymers include, rubbers and hydrogels.

1.5 Free Radical Polymerization (FRP)

Free radical polymerization (FRP) is one of the most used polymerization techniques due to its relative insensitivity to impurities, moderate reaction temperatures, and the multiple polymerization processes available.[14] There are certain disadvantages that also come along with this technique such as poor control of molecular weight and molecular weight distrubtion.[14] FRP is a type of chain growth polymerization which means the polymeric chain grows in successive addition of monomer units.[10]

The 4 main steps in FRP include:

1. **Initiation:** A reactive site is formed which initiates the polymerization.[14]
2. **Propagation:** Monomer units are added one by one to the active chain end and the reactive site is regenerated after each monomer unit is added.[14]
3. **Transfer:** Active site is transferred to a monomer, initiator, polymer, or solvent which results in a terminated molecule and a new active site for propagation.[14]
4. **Termination:** Eradication of active sites leads to termination of the growth of the chain. This can happen in two ways combination or disproportionation.[14]

Shown below is **Figure 1.8** for better representation of these steps.

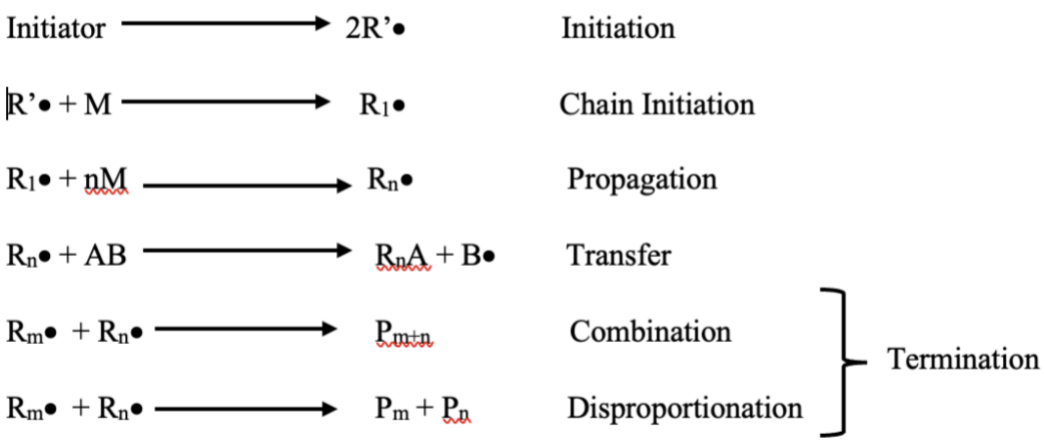

Figure 1.8: Scheme for FRP. R• represents a free radical capable of initiating propagation; M represents a monomer. R_m• and R_n• represents a propagating radical chain with a degree of polymerization of m and n respectively. AB is a chain transfer agent; Pn + Pm represent terminated macromolecules.[14]

There are limitations to FRP such as the little control over the molar mass distribution due to diffusion-controlled termination reactions between growing radicals and there is no possibility of block copolymers or other chain topologies due to the short life span of the propagating chain

which is usually in the range of 1 second.[14] To tackle these disadvantages a subgroup of FRP called living/controlled radical polymerization (LRP) was developed which has no termination and is only stopped when there is no more monomer, and the reaction can continue upon addition of monomer units.[14] The three subgroups in LRP include nitroxide mediated polymerization (NMP), atom transfer radical polymerization (ATRP), and reversible addition-fragmentation chain transfer (RAFT).[14]

1.6 Hydrogels

Hydrogels are 3 dimensional polymeric networks that can absorb large amounts of water while also keeping their structural integrity.[9] The water holding capacity of hydrogels is attributed to the presence of hydrophilic groups on the polymer chain.[10] Hydrogels can hold anywhere from 10 to 1000 times excess of water compared to the weight of the hydrogels. This depends on the number of hydrophilic groups as well as cross-linking density of hydrogels.[10] The higher the number of hydrophilic groups the more water the hydrogel can hold, while an increase in crosslinking density can cause a decrease in swelling due to the decrease in flexibility of the hydrogel structures.[10] Hydrogels are used in a wide variety of applications including biomedical applications such as drug delivery, tissue engineering and cryopreservation. The ability to modify them in many ways such as the monomer composition or use of different crosslinkers make them a great candidate for these biomedical applications. Hydrogels have shown many useful properties such as biocompatibility, potential responsiveness to small environmental changes, ability to store functional chemicals and nanoparticles, and many more.[9] One important property of polymers and hydrogels that is used for phycological applications is a lower concentration solution temperature (LCST) of around 37°C. LCST is the temperature at which the polymer undergoes a change in conformation such as from random coils to a collapsed state as shown in **Figure 1.9**.[18]

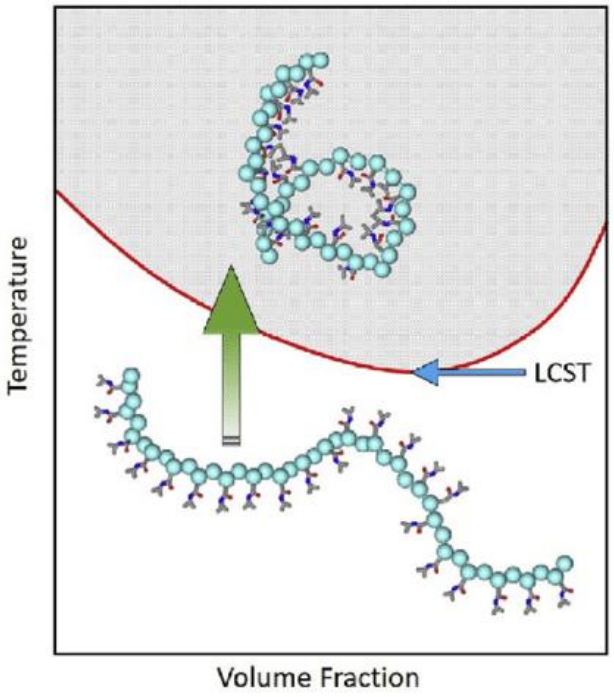

Figure 1.9: Schematic illustration of the transition behavior of LCST thermo-responsive polymers; the red line represents the macroscopic phase transition. This shows the behavior of an LCST polymer, such as poly(N-isopropylacrylamide) in water.

When the polymer/hydrogel is heated in aqueous solutions at the LCST, the polymer chains collapse and display intramolecular hydrophobic interactions.[18] These interactions can enhance the phase separation of polymer chains from aqueous solution[16], hence yielding stimuli responsive properties to the polymers and hydrogels. Below LCST, the polymers are soluble and above LCST, they become increasingly hydrophobic and insoluble which leads to gel formation.[10]

Hydrogels can be classified into two groups depending on the type of crosslinking: permeant hydrogels and physical hydrogels.[10] Permanent hydrogels contain covalent bonds formed during the cross-linking reaction while physical hydrogels are formed from physical interactions such as molecular entanglement, ionic interaction, and hydrogen bonding among the polymeric chain.[10] The hydrogels can also be classified as conventical or stimuli responsive

hydrogels.[10] Conventional hydrogels have no change in swelling behaviour with a change in pH, temperature, or electric field while stimuli responsive hydrogels are the opposite as the swelling will change with a change in pH, temperature or electric field.[10] Those are two ways that hydrogels can be classified but there are many more classification which can be seen in **Figure 1.10**.

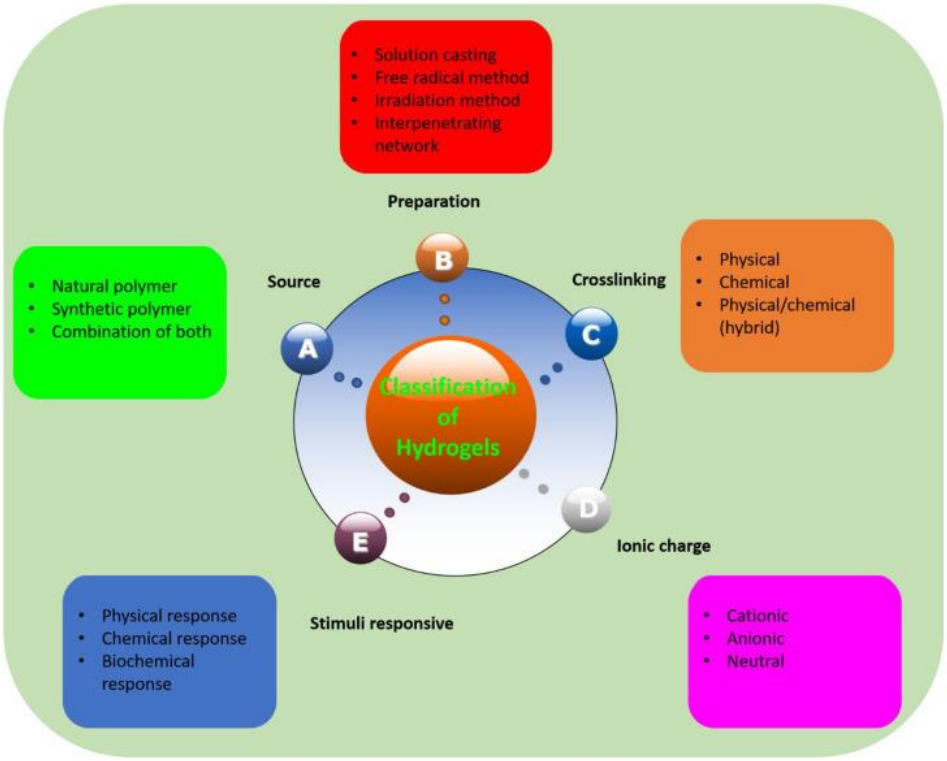

Figure 1.10: Classification of hydrogels.[22]

One method of classification is preparation as seen in the above figure and hydrogels which as stated before are just hydrophilic polymeric networks crosslinked to produce an elastic structure can be synthesized anyway a regular cross-linked polymer can.[21] This is why copolymerization/cross-linking free-radical polymerizations are commonly used to produce hydrogels by reacting hydrophilic monomers with multifunctional cross-linkers.[21] Other methods such as bulk, solution and suspension polymerization can be used as well.[21] FRP is mentioned and explained in section 1.5. Our hydrogels are classified as a physical response hydrogel due to them

being shear-thinning and have a physical response to shear stress. This is further explained in the next section.

1.6.1 Shear-thinning Hydrogels

Shear-thinning hydrogels are a sub-group of hydrogels that show the property of shear-thinning. Shear-thinning hydrogels can be injected and flow by the application of shear stress and quickly self-heal after that shear is removed.[19] **Figure 1.11** shows below a great overview of shear-thinning hydrogels.

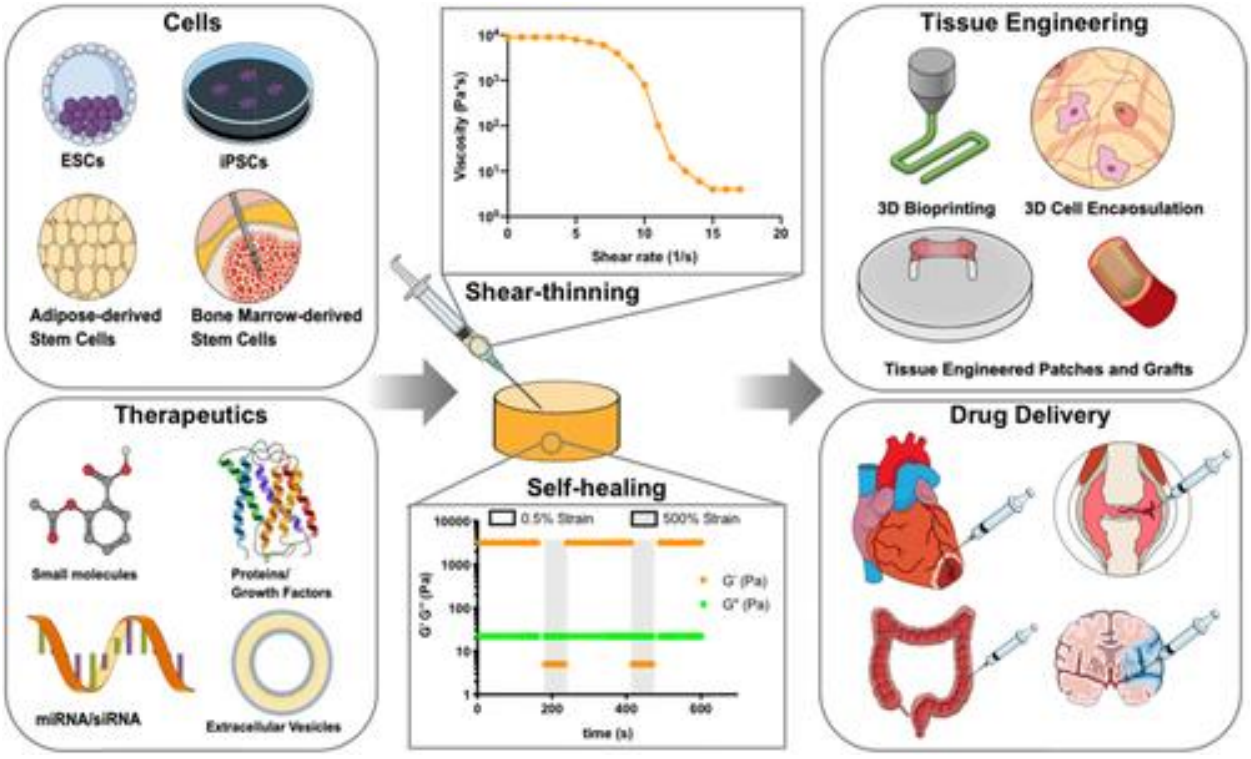

Figure 1.11: Shear-thinning hydrogels and their applications.[27]

These hydrogels show great use in tissue engineering and drug delivery as they can be prepared as stable formulations beforehand and undergo the process of shear-thinning during injection and then recover with self-healing post-injection.[19] There has been much research into these hydrogels as they show great promise for use in the above-mentioned categories. With the versatility of

hydrogels as well as the many different monomers and crosslinkers available to be used in the fabrication of shear-thinning hydrogels the possibilities are endless. With respect to drug delivery, these hydrogels are promising as they can encapsulate payloads and inject through needles without clogging and recover to their initial state.[19] These hydrogels as well provide greater concentrations of therapeutics at desired sites of action while minimizing the side-effects of systemic delivery.[19]

1.7 Project Description

1.7.1 Objectives

- Synthesis of shear thinning hydrogels with different compositions of monomers (B5AMA and DEGMEM) and crosslinkers (OXAS, EGDMA, and diallyl disulfide)
- Characterisation these hydrogels with
    - Dynamic light scattering (DLS)
    - Swelling kinetics
    - Zeta-potential
    - Lower critical solution temperature (LCST) determination
    - Injectability Studies

1.7.2 Description of Objectives

The first objective of this project is the synthesis of shear thinning hydrogels using B5AMA, di(ethylene glycol) methyl ether methacrylate (DEGMEM) and various crosslinkers such as ethylene glycol dimethacrylate (EGDMA), (3,9-divinyl-2,4,8,10-tetraoxaspiro[5.5]undecane) (OXAS) and diallyl disulfide to test their injectability through a syringe. More than 30 different compositions of hydrogels with varying monomer and

crosslinker concentrations were prepared. A handful of compositions that showed good shear thinning behavior/injectability through a syringe were further tested for by different characterization techniques including dynamic light scattering (DLS), water absorbance studies, zeta-potential, and swelling kinetics. All the data was collected and compared to literature values for similar hydrogels in this field.

2 Experimental

2.1 Materials

Ethylene glycol dimethacrylate 98%, EGDMA), 3,9-Divinyl-2,4,8,10-tetraoxaspiro[5.5]undecane (98%, OXAS), di(ethylene glycol) methyl ether methacrylate (95%, DEGMEM), 3-(Trimethylsilyl)-1-propanesulfonic acid sodium salt (97%, TMSPA), d-penatolactone (99%), potassium persulfate (99%, KPS), diallyl disulfide (80%), 4,4′-azobis(4-cyanopentanoic acid) (98%, ACVA), N,N,N',N'-tetramethylethylenediamine (99.5%, TEMEDA), triethylamine (99%, TEA) and hydroquinone were purchased from Sigma Aldrich. Methanol (99.9%) and acetone were purchased from Fisher Scientific. Ethanol anhydrous was purchased from Commercial Alcohols. AEMA was synthesized in the laboratory according to previously reported procedures[23].

2.2 Synthesis of B5AMA

2.2.1 Small Batch Method

The synthesis of the monomer B5AMA was carried out by a previously reported procedure.[2] 4.0g of synthesized AEMA along with 22mL of TEA, 14mL of methanol and a few flakes of hydroquinone were added to a round-bottom flask and stirred, once AEMA is dispersed 3.79g of d-pantolactone was added and a nitrogen head apparatus was attached, and the solution was left to stir overnight. The next day the solution was then roto evaporated to remove impurities and excess of solvents. Then 50mL of acetone was added, and the solution was stirred and then vacuum filtrated to remove the precipitated triethylamine hydrochloride. The filtrate was kept, and the white solid by-product was placed back into the flask and 30mL of acetone was added and then was left to stir for 30 minutes. This solution was then vacuum filtrated again and the filtrate was combined with the previously acquired filtrate. The filtrate was observed to see if any precipitant

was visible and if some was visible the solution was vacuum filtered again, but if no precipitate was visible the filtrate was roto evaporated down to roughly 5mL. This was then ran through a column with 100mL of acetone and roughly 20mL of silica gel. The column was ran with 200mL of acetone. All eluent was recovered, and this was then roto evaporated again down to 5mL. This was then run through a column made up of 500mL of acetone and 250mL of silica. The column was ran with enough acetone as needed. The dead volume of the column was approximately 150mL. Fractions were then collected in test tubes every 20mL while checking with running thin layer chromatography (TLC). B5AMA usually eluted around the fractions 5-20. After checking with last TLC to see no more B5AMA was eluting all test tubes containing B5AMA were added to another round-bottom flask and roto evaporated until no acetone was left and the final product was left under vacuum, and a sample was taken for NMR.

2.2.2 Big Batch Method

This method is almost the same as above except all values of AEMA, TEA, methanol, pantolactone, and acetone were doubled and only one bigger column is used rather than 2, which was made with roughly 700mL of silica with 1200mL of acetone. The dead volume of the column was roughly 500mL and fractions were collected roughly every 40mL. The elute came out in fractions 20-60 depending on the synthesis. See **Figure 2.2** for perspective of column. The reaction scheme of B5AMA is shown in **Figure 2.1.**

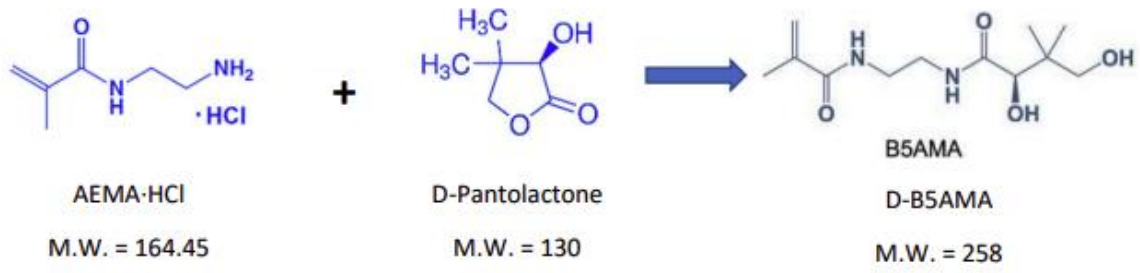

Figure 2.1: Reaction scheme for B5AMA.

Figure 2.2: Column being ran for a big batch of monomer B5AMA.

2.3 Synthesis of hydrogels

Two degasification methods were used: ultrasonic bath method and freeze thaw method both of which are explain below in sections 2.3.1 and 2.3.2. The solvent used in the synthesis of all hydrogels was 50:50 ethanol:dionized water. All hydrogels had similar procedures except for a few differences. **Figure 2.3** shows the general scheme of how each hydrogel was prepared.

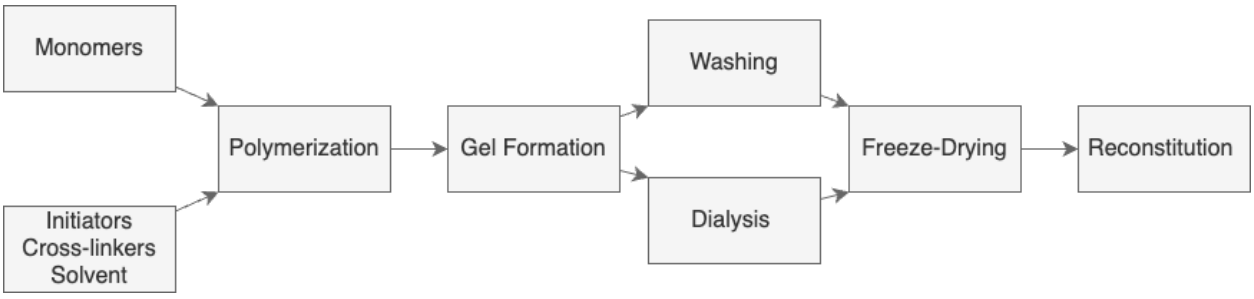

Figure 2.3:Scheme for synthesis of hydrogels.

The main difference is that when using the ultrasonic bath method, no dialysis was preformed and rather the hydrogels would be washed. When using the freeze-thaw method, dialysis was used rather than washing. Shown below in **Figure 2.4** are the chemical structures and names of all molecules used for this project.

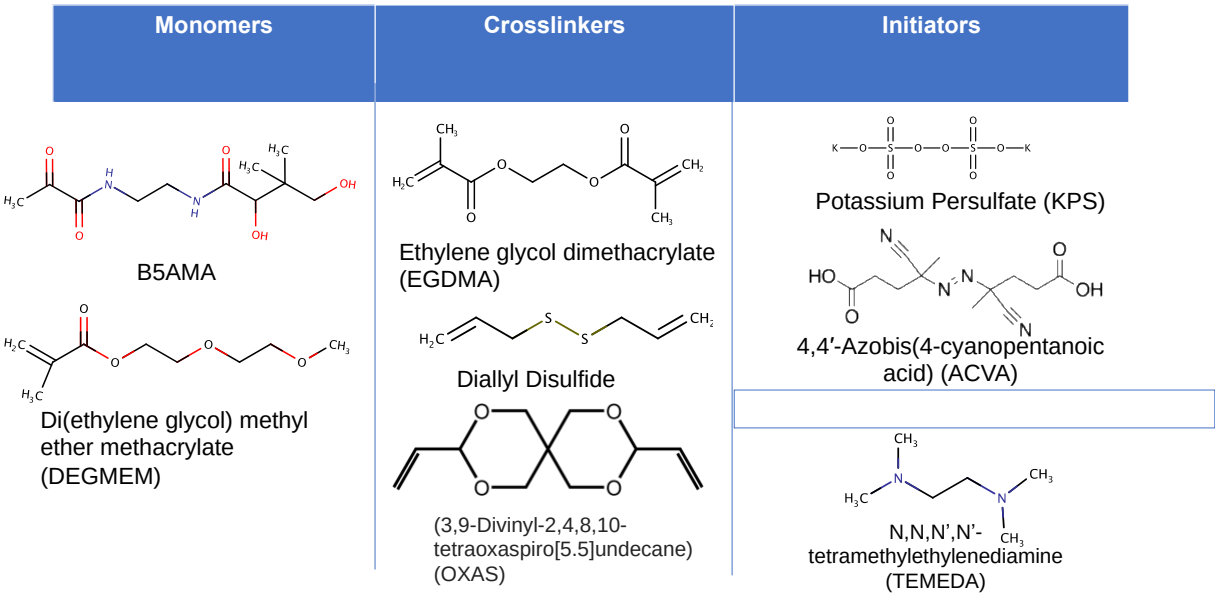

Figure 2.4: Chemical structure and names of all molecules used in the synthesis of hydrogels in this project.

2.3.1 Ultrasonic bath Method

The compositions of shear thinning hydrogels is shown in **Table 2.1** and **Table 2.2** were all done using the following method.

Table 2.1: Compositions of hydrogels synthesized using the ultrasonic degasification method. * Everything after these were made with filtered DEGMEM and EGDMA.

Reaction	$m_{reactions}$ mg	%w monomer	%w Solvent 50:50 EtOH:H_2O	%w B5AMA	%w DEGMEM	% mol EGDMA	% mol KPS	% mol TEMEDA
KW-1-1	1200	15	85	7.5	7.5	7.0	7.0	10.0
KW-1-2	1200	15	85	7.5	7.5	4.0	7.0	10.0
KW-8-1	12000	15	85	7.5	7.5	7.0	3.5	5.0
KW-8-2	12000	15	85	7.5	7.5	4.0	3.5	5.0
KW-9-1	6200	15	85	7.5	7.5	7.0	7.0	10.0
KW-9-2	6200	15	85	7.5	7.5	4.0	7.0	10.0
KW-10-1*	6200	15	85	7.5	7.5	4.0	3.5	5.0
KW-10-2*	6200	15	85	7.5	7.5	7.0	3.5	5.0
KW-17-1	2000	15	85	15	0	4.0	3.5	5.0
KW-18-1	2000	15	85	10	5	4.0	3.5	5.0
KW-19-1	2000	15	85	5	10	4.0	3.5	5.0
KW-20-1	2000	15	85	0	15	4.0	3.5	5.0

Table 2.2: Composition of hydrogel synthesized using ultrasonic degasification method.

Reaction	B5AMA/DEGMEM mol	Diallyl disulfide % mol	AIBN % mol	Solvent ml 50:50 H_2O:ACN
KW-2-1	1.37	4.00	6.0%	40 ml

EGDMA and DEGMEM would be filtered using a glass pipette filled with glass wool and silica. Then EGDMA and KPS were separately made into solution. EGDMA was dissolved in 50:50 ETOH:H_2O and KPS was dissolved in deionized water. The reaction was performed in 25ml vial. First B5AMA, DEGMEM, EGDMA, and ETOH:H_2O were added to 25 mL vial. KPS was added last as it is the initiator. The solution was then stirred to make sure it was homogenous and taken to the ultrasonic bath. The vial, with the cap off, was then placed in a small beaker with roughly 20-30mL of water and placed in the ultrasonic bath for 5 minutes. In the last 30 seconds the TEMDA was added as a catalyst and after 30 seconds the vial was taken out and left with the cap on to gel. Typically, overnight. The next day the sample was washed 3 times with deionized water and left again overnight in water to wash. The next day the purified sample was freeze dried. The sample was prepared for the freeze dryer by first using a kim wipe with a plastic band in place to keep the kim wipe on top of the vial as a cover. The sample was then placed in a beaker and submerged in a approximately 200-300mL of liquid nitrogen for 15 minutes to freeze. After the 15 minutes the sample was placed in the freeze dryer and left for 1-2 days. The sample was then taken out of the freeze dryer and was ready to use experiments.

2.3.1.1 Samples used for Swelling Kinetics

Samples prepared for use in swelling kinetics were prepared the same way as the method mentioned in 2.3.1 but rather than being placed in vials and left to gel the samples were placed into 5mL syringes as shown in **Figure 2.5.**

Figure 2.5: Hydrogels placed in syringes after ultrasonic bath for use in swelling kinetics.

2.3.2 Freeze-Thaw Method

Table 2.3: Compositions of all hydrogels synthesized using the freeze-thaw.

Reaction	$m_{reactions}$ mg	%w monomer	%w Solvent 50:50 EtOH:H_2O	%w B5AMA	%w DEGMEM	% mol OXAS	% mol ACVA
KW-7-1	3000	25	75	12.5	12.5	6.0	0.3
KW-7-2	3000	25	75	12.5	12.5	4.0	0.3
KW-21-1	3000	25	75	12.5	12.5	10.0	0.3
KW-21-2	3000	25	75	12.5	12.5	8.0	0.3
KW-25-1	4000	25	75	12.5	12.5	6.0	0.3
KW-25-2	4000	25	75	12.5	12.5	4.0	0.3
KW-27-1	3000	25	75	25.0	0.0	6.0	0.3
KW-27-2	3000	25	75	20.0	5.0	4.0	0.3
KW-27-3	3000	25	75	15.0	10.0	10.0	0.3
KW-28-2	2000	25	75	12.5	12.5	8.0	0.3
KW-29-1	2000	15	85	7.5	7.5	10.0	0.3
KW-29-2	2000	15	85	7.5	7.5	8.0	0.3
KW-30-1	2000	25	75	20.0	5.0	10.0	0.3
KW-30-2	2000	25	75	20.0	5.0	8.0	0.3
DFC-722-2	2000	25	75	20.0	5.0	8.0	0.3
KW-31-1	2000	25	75	25.0	0.0	10.0	0.3
KW-31-2	2000	25	75	25.0	0.0	8.0	0.3
KW-34-2	2000	25	75	25.0	0.0	8.0	0.3
KW-37-3	3000	25	75	0.0	25.0	10.0	0.3
KW-37-4	3000	25	75	0.0	25.0	8.0	0.3
KW-44-1	3000	25	75	12.5	12.5	0.0	0.3
KW-44-2	3000	25	75	20.0	5.0	0.0	0.3

DEGMEM would be filtered using a glass pipette filled with glass wool and silica. Then OXAS and ACVA were made into solutions with 50:50 ETOH:H_2O. B5AMA, DEGMEM, OXAS and solvent are then all added into small 5mL round bottom flasks with small stir bars. The samples were then subjected to three freeze thaw cycles to remove any oxygen, before the polymerization can be performed. Briefly, approximately 2 liters of liquid nitrogen was obtained and approximately 1 liter was placed into the vacuum canister and the rest was kept to freeze the samples. AVCA was added last to the reaction flask as it was the initiator and then the samples

containing flasks are attached to nitrogen heads and attached to the nitrogen lines. Vacuum grease was used in all openings to ensure the round bottom flasks do not get stuck to the nitrogen heads. The samples are then frozen in liquid nitrogen under nitrogen gas for 5 minutes and then the nitrogen gas was closed, and the vacuum was opened and left on for 5 minutes. After 5 minutes the vacuum is closed, and the nitrogen gas was turned back on and the samples were placed in a water bath to thaw. This procedure is repeated another two times. After the last cycle and the samples are completely thawed then placed in an oil bath at 70 °C and left overnight. The next day the samples were taken out and dissolved in deionized water and put into dialysis tubes for 2-3 days. After dialysis the samples were then put in the freeze dryer with the same method as explained in section 2.3.1. After 2-3 days in the freeze dryer the samples were ready for use in experiments.

2.4 Characterization methods

2.4.1 Swelling Kinetics Sample Preparation

9 samples were weighed and then placed in 5mL vials containing water. The 9 samples were each left for different time points ranging from 5 minutes to 24 hours. Once a specific time point was reached the sample was taken out and the water strained, and the sample was patted as dry as possible and then weighed again. A weight ratio of hydrogels before adding to water (W_o) and after absorbing the water (W_t) provided the swelling ratio. The swelling ratio was used to show how much the hydrogel had swelled. Once all data had been recorded the data was plotted in excel to visualize a general trend.

2.4.2 Dynamic Light Scattering (DLS) Sample Preparation

Samples prepared for DLS were first crushed as fine as possible in a mortar and pestle. 5mg was then weighed out and placed into a 5mL vial and 1mL of deionized water was added to

give a concentration of 5mg/mL for each sample. Samples were then transferred into a 1mL cuvette and placed in the NanoBrook 90Plus PALS. The measurements were taken at every 3°C starting at 25°C going up to 61°C. Once all data is obtained it is plotted in excel.

2.4.3 Absorption Studies

Samples for absorbance studies were prepared using 5mg of hydrogel with 1mL of water for a concentration of 5mg/mL. The sample were then be placed in a water bath with a temperature monitored hot plate and temperatures were taken starting at 25°C going up by 5°C until 60°C was reached. UV-Vis spectroscopy was performed to measure LCST of hydrogels. Deionized water was used as a blank. The samples, at different temperatures, were taken and were placed in the Hewlett Packard 8453 spectrophotometer. The change in absorbance was measured at 625nm. After all data was obtained it was plotted on a graph in Excel.

2.4.4 Zeta-Potential Sample Preparation

Zeta potential used the same initial preparation as above but used a concentration of 1mg/mL rather than 5mg/mL. Once the samples were prepared these were taken to the NanoBrook 90Plus PALS and was placed in a 5ml cuvette and then was placed in the solvent-resistant electrode used to determine zeta potential for analysis.

3. Results and Discussion

3.1 Synthesis of B5AMA

B5AMA as explained before was one of the main monomers used for all experiments so it was synthesized several times over the course of this project using a previously reported method.[2] A table of all trials can be seen in **Table 3.1**.

Table 3.1: All synthesis of B5AMA performed with % Yield. *NMR spectra can be found in appendix A.

Name	**% Yield**	**NMR***
KW-5-1	82.22	Figure 7.1
KW-26	83.61	Figure 7.3
KW-32	62.55	Figure 7.4
KW-33	69.52	Figure 7.5
KW-36	89.13	Figure 7.6
KW-40	56.45	Figure 7.7
KW-45	61.13	Figure 7.9

All syntheses were successful with all yields being above 50%. Lower yields can be attributed to lab error such as air bubbles in column, not roto evaporating enough solvent off and still having impurities after vacuum filtration. But overall yields were sufficient, and enough product was always obtained for use in multiple experiments.

3.2 Synthesis of Hydrogels with EGDMA and Diallyl Disulfide Crosslinkers

Many different compositions of hydrogels were tried with two crosslinkers EGDMA and diallyl disulfide. The Hydrogels made for this section are shown in **Table 2.1**. and **Table 2.2**. All hydrogels used in these experiments were prepared using the ultrasonic degasification method.

3.2.1 Characterization

3.2.1.1 Injectability Studies

Our first goal was to obtain shear-thinning hydrogels with a focus on being able to inject the hydrogel through a syringe. Our first hydrogels synthesized had the compositions shown in **Table 2.1** as KW-1-1 and KW-1-2 and **Table 3.2**. After synthesis each hydrogel was reconstituted in deionized water, shown in **Table 3.3**.

Table 3.2: Reconstituted concentrations.

Reconstitution	**Hydrogel, mg**	**Water, µL**
KW-1-1 (7% EGDMA)	20	113
KW-1-2 (4% EGDMA)	20	113
KW-2-1 (d	49	50

Then each hydrogel was subjected to being put through a 1 mL syringe. KW-1-1 and KW-1-2 which differed only in amount of crosslinker used with 7% and 4% mol EGDMA respectively. They each were found to require excessive force to push through the syringe but once that force was reached the hydrogel did flow out the syringe and after 1-2 minutes the hydrogel became very hard as it kept its shape. This confirmed that it did in fact have shear-

thinning properties. KW-2-1, which was made using the diallyl disulfide crosslinker, after reconstituted was found to be not viscous enough to test.

3.2.1.2 Swelling Kinetics

The swelling kinetics in this project were used to see how much our hydrogels swelled, to in turn see how much drug we would be able to load into the hydrogel if they were to be used for drug delivery purposes. Solubility problems were run into as seen in **Figure 3.1** where a white precipitate would form.

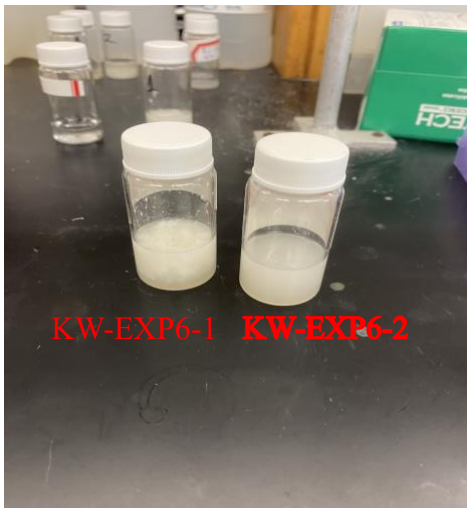

Figure 3.1: Hydrogels after ultrasonic bath method showing white precipitate.

This was attributed to the gelation happening too quickly after the ultrasonic bath, so the amount of catalyst (TEMDA) was reduced from 10% mol to 5% mol.

As seen in **Figure 3.2,** with lower amount of catalyst loading, the hydrogels came out much clearer with no precipitate. They have the same composition as KW-10-1 and KW-10-2.

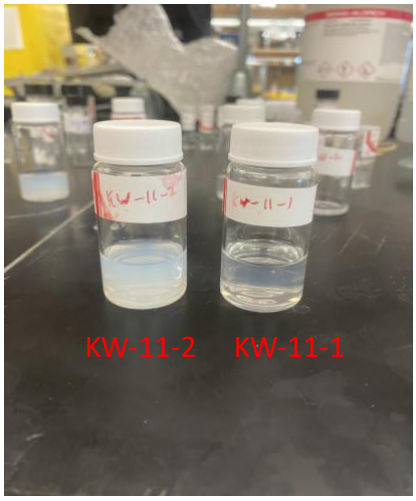

Figure 3.2: Hydrogels KW-11-1 and KW-11-2 after ultrasonic bath and gelation.

After the issue of solubility was solved, hydrogels were prepared for swelling studies. The first hydrogels used for this were KW-10-1 and KW-10-2 which compositions can be seen in **Table 2.2**. KW-10-1 which had 4% mol EGDMA and KW-10-2 which had 7% mol EGDMA where used in initial experiments and can be their data can be seen in Appendix B. All swelling kinetics were done with deionized water at neutral pH. This initial experiment showed that KW-10-2 (7% EGDMA) swelled up more than KW-10-1 (4% EGDMA) so more extensive experiments were conducted using the same composition as KW-10-2. Shown in **Figure 3.3** is the average data for swelling kinetics done on KW-13-1 and KW-15-1 which all had the same composition as KW-10-2. It was found that the hydrogel was able to swell up on average to a maximum of 8x its original mass. Comparing this to recent literature in a paper by Diramio et al[26]. it was found that their poly(ethylene glycol) methacrylate (PEG-MA)/dimethacrylate (PEG-DMA) hydrogels swelled up to 7x their mass for low MW crosslinkers and around 10x their mass for high MW crosslinkers[26]. This is reasonably close to our data found for this experiment and shows that our

hydrogels could take up to 8x their mass which could be useful for future use in drug-delivery studies. Other swelling kinetics were done but the data obtained was not enough to get a useful graph, they can be seen in Appendix B. the individual data and graphs for KW-13-1 run 1 and 2 as well KW-15-1 can also be seen in Appendix B.

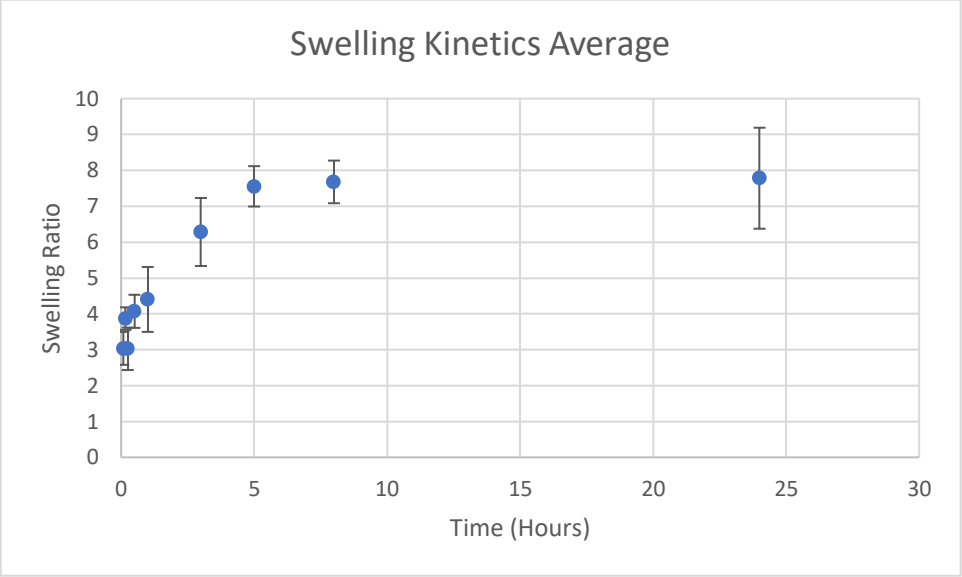

Figure 3.3: Graph for average of swelling kinetics experiments 1, 2, and 3.

3.3 Synthesis of Hydrogels with OXAS Crosslinker

Many different compositions of hydrogels were tried with crosslinker OXAS. The Hydrogels made for this section were shown in **Table 2.3**. They were made using the freeze-thaw degasification method.

The focus for these hydrogels was to obtain hydrogels that showed LCST which was able to be found using both DLS and absorbance studies.

3.3.1 Characterization

3.3.1.1 DLS

The compositions for DLS analysis were given in **Table 2.3**. The compositions all stayed the same with respect to monomer composition and only varied in % mol OXAS used. 4% (KW-7-2), 6% (KW-7-1), 8% (KW-21-2), and 10% (KW-21-1) were all used to see if there was a difference in each and which of these would show LCST at 37°C.

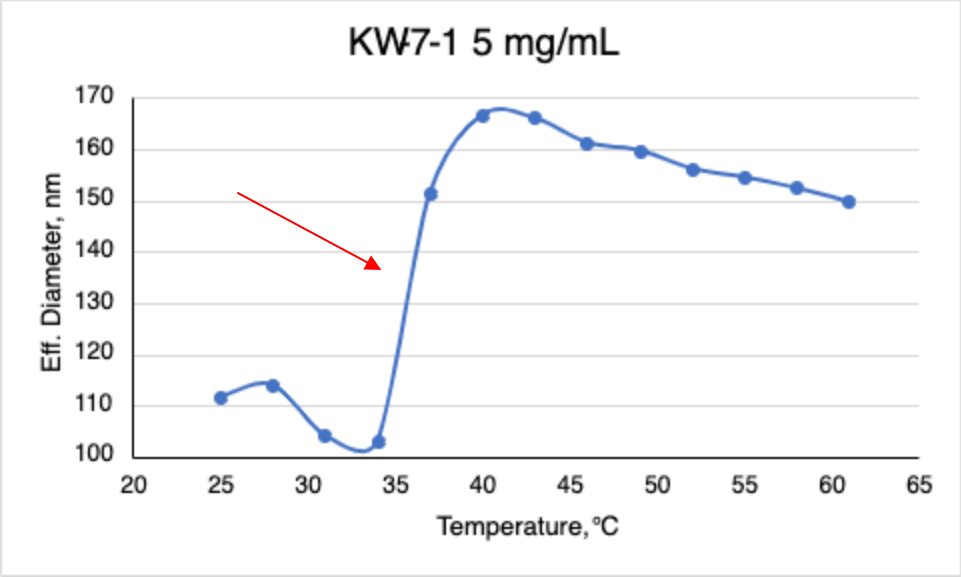

Figure 3.0.4: Graph of DLS data for KW-7-1.

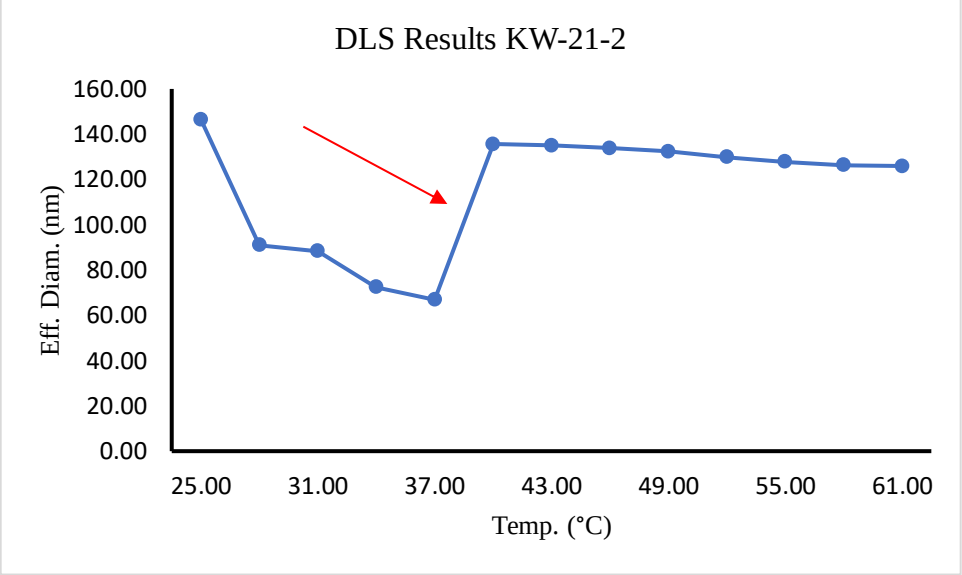

Figure 3.5: Graph of DLS data for KW-21-2.

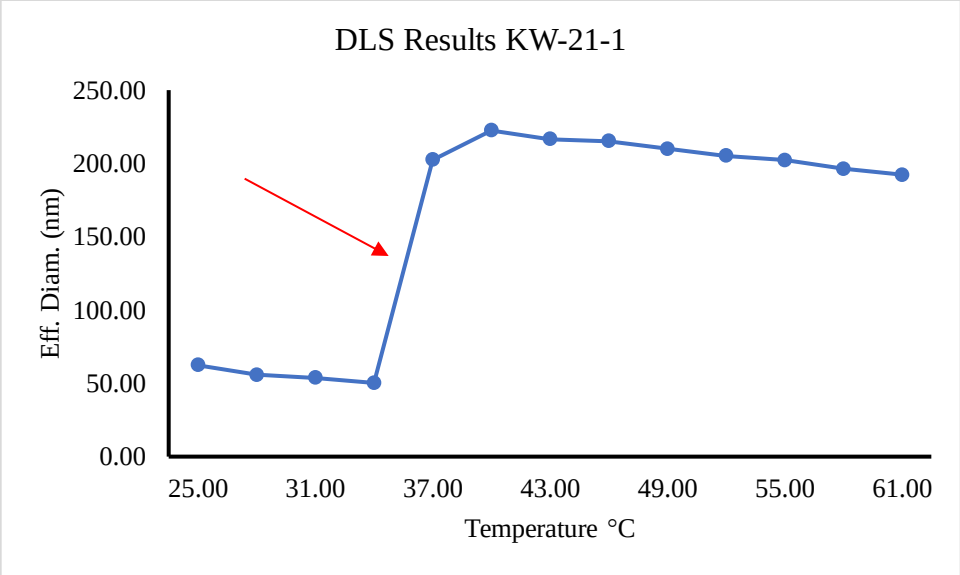

Figure 3.6: Graph of DLS data for KW-21-1.

To begin, it should be noted that KW-7-1, KW-7-2, KW-21-1, and KW-21-2 were measured in a single run on the DLS, with three measurements taken at the same temperature. In contrast, for all other samples, the data was obtained by conducting three separate DLS experiments, with only one measurement taken at each temperature. It's worth mentioning that the first two runs of KW-34-2 were done using the same method as KW-7-1, KW-7-2, KW-21-1, and KW-21-2. The method was changed due to taking up to 6 hours in one day to complete measurements. Key results to note is for KW-7-1, KW-21-2, and KW-21-1 which had 6%, 8% and 10% mol OXAS respectively, all showed LCST of around 37°C (indicated by the red arrows), which is body temperature. This is a very interesting and useful property that makes these hydrogels useful for physiological applications. These hydrogels are currently being used in the research of cryopreservation of cells in the Ahmed lab. KW-7-2 (4% OXAS) had a very inconsistent DLS graph which can be seen in Appendix C which showed that lower amounts of OXAS did not show an LCST of 37°C.

KW-27-1, KW-34-2, KW-27-2 and DFC-722-2 were synthesized for DLS analysis to see if these hydrogels showed LCST with a lower amount of DEGMEM and higher amount of B5AMA. KW-27-1 and KW-34-2 were made completely with B5AMA and no DEGMEM with 6% and 8% mol OXAS respectively. While KW-27-2 and DFC-722-2 were made with 20%w/w B5AMA and 5%w/w DEGMEM with 4% and 8% mol OXAS respectively. None of these exhibited an LCST of 37°C and rather had a value closer to 50°C for all. The data for all these can be seen in appendix c. This showed that a higher amount of DEGMEM was required to give the LCST properties desired for these hydrogels.

3.3.1.2 Absorption Studies

Another study used to analyze hydrogels for LCST was absorption studies, which were only done on samples KW-7 and KW-21 due to it requiring excessive time and equipment to run.

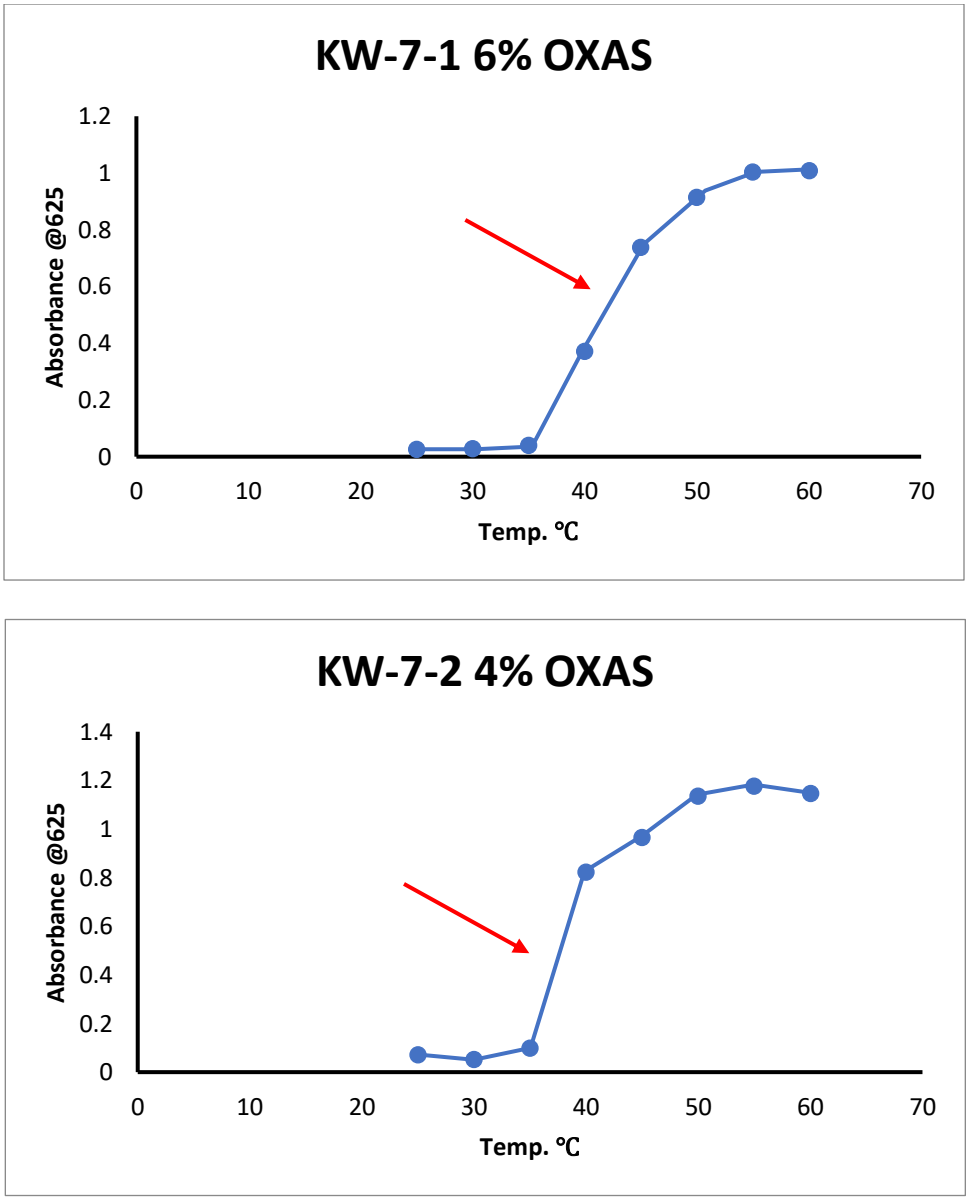

Figure 3.7: Graphs of absorbance data for KW-7-1 (6% OXAS) and KW-7-2 (4% OXAS).

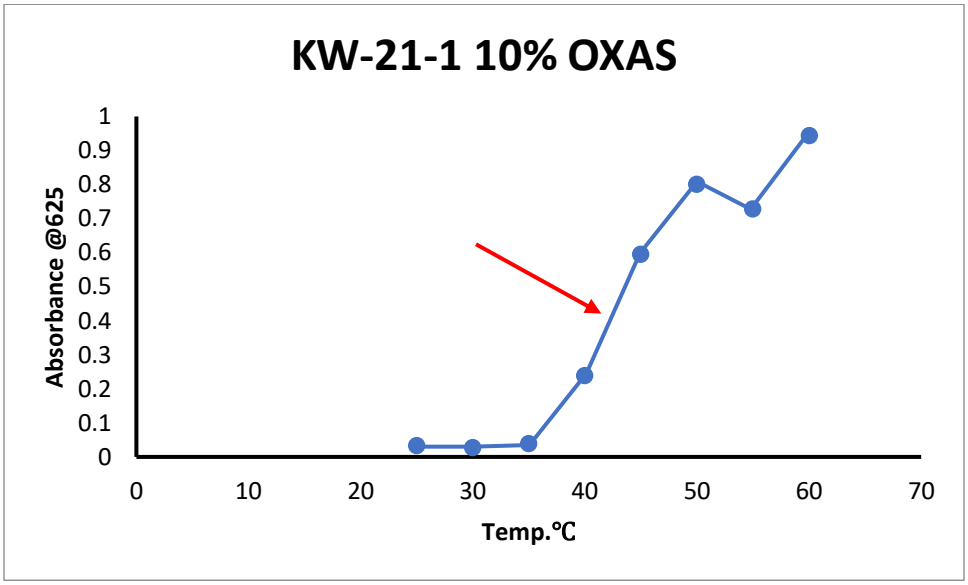

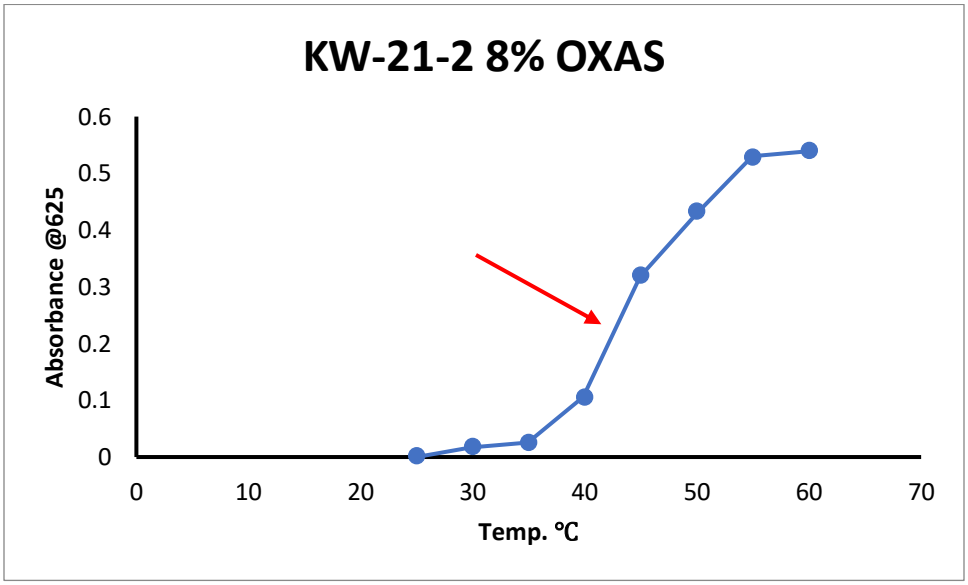

Figure 3.8: Graphs of absorbance data for KW-21-1 (10% OXAS) and KW-21-2 (8% OXAS).

The data shows that for KW-7 and KW-21 they each had a their most significant jump in between 35-40°C (as indicated by the red arrows) which indicates that 37°C could be a possible LCST. This showed, unlike the DLS, that KW-7-2 which had the lowest percentage of OXAS at

4% could possibly show LCST at 37°C. Absorption studies were found to be less accurate then DLS analysis due to there being more opportunity for human error due to having to take the sample out of the bath and back in for every measurement. But overall, the data was still consistent with other found in previous experiments.

3.3.1.3 Zeta-Potential

The Zeta-Potential was taken to find the surface charge of our hydrogels to see whether they had a positive, negative, or neutral charge at a neutral pH. The hydrogels surface charge is found to be neutral if the charge falls within the range of -10mV to +10mV and is considered strongly anionic and strongly cationic when found above -30mV and +30mV respectively[19]. Neutral charged hydrogels would show they would have no interacting with surrounding molecules in the physiological system. If the hydrogels were found to be negative or positive, they would affect the tendency of the nanoparticles in the hydrogels to permeate membranes[19]. Positive particles are found to display more toxicity associated with cell wall distrupition[19].

The compositions that were used were the same as the ones used for the DLS analysis and were given in **Table 2.2**.

Table 3.3: Data for zeta-potential of KW-28-2.

	KW-28-2 Zeta-Potential		
Run	1	2	3
Zeta-Potential (mV)	-7.49	-7.46	-8.31
Graph	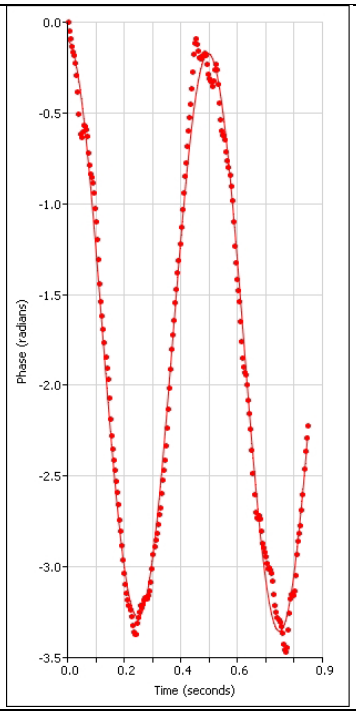	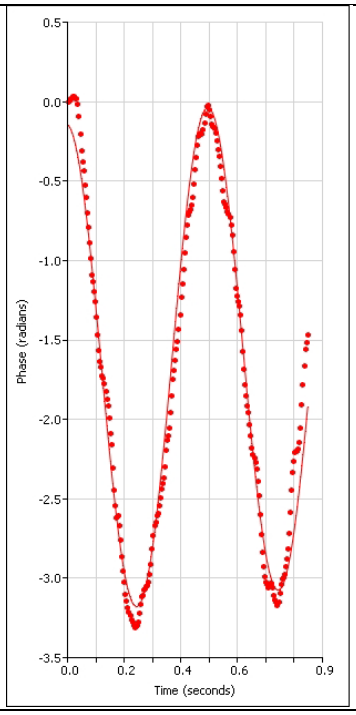	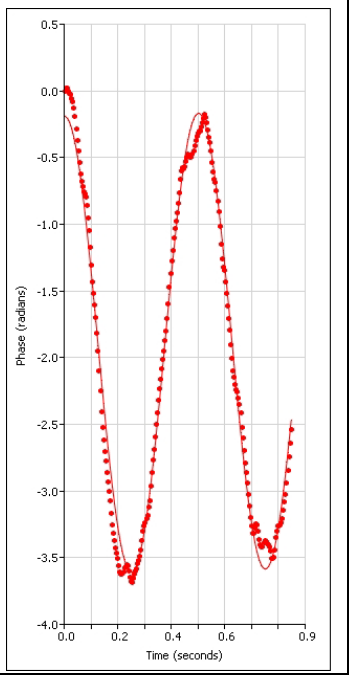

KW-28-2 (8% OXAS) was found to have an average zeta-potential of -7.75mV which fell into -10mV to +10mV range which indicates the hydrogel has a neutral charge. All other hydrogels analyzed had zeta-potential values that fell into the -10mV to +10mV range as well which is considered a neutral charge. Having a neutral charge shows that the surface of the polymer is neutral and is unlikely to interact with surrounding molecules. This data shows that these hydrogels show the relevant properties to be used in the future in physiological applications. All other data can be found in Appendix E.

4. Conclusion

B5AMA was synthesized multiple times and used in the synthesis of hydrogels. More than 30 different compositions were prepared using various monomer compositions and three different crosslinkers; EGDMA, OXAS, and diallyl disulfide, which resulted in hydrogels with varying physical properties. The properties were characterized through multiple techniques such as dynamic light scattering (DLS), absorption studies, injectability testing, zeta-potential, and swelling kinetics.

The first set of hydrogels were synthesized using the EGDMA crosslinker and tested for injectability. The results showed that these hydrogels were shear-thinning and could be injected through a syringe and maintain their shape after injection. Furthermore, the hydrogels were found to have a high water-holding capacity, swelling up to 8 times their weight.

The subsequent hydrogels were synthesized using the OXAS crosslinker, and multiple compositions were prepared and characterized using DLS, absorbance studies, and zeta-potential analysis. These hydrogels exhibited an LCST at 37°C, as observed through DLS, which makes them a promising candidate for biomedical applications such as cryopreservation of cells. This was further confirmed by an absorbance test, which showed the OXAS crosslinked hydrogels have an LCST between 35-40°C. Moreover, the zeta-potential of these hydrogels was found to be neutral range.

Overall, the successful synthesis of B5AMA and its use in the production of hydrogels with varying physical properties is a significant advancement in the field of biomedical research. The ability of these hydrogels to exhibit an LCST at physiological temperatures makes them highly promising for various biomedical applications, including but not limited to, cryopreservation of cells, drug delivery, and tissue engineering. Moreover, the use of different crosslinkers and

monomer compositions allowed for the synthesis of hydrogels with unique properties, which could be tailored to specific applications. Therefore, the successful synthesis and characterization of these hydrogels offer promising possibilities for the development of novel and improved biomedical technologies in the future.

5. Future Work

Based on the data collected and the observation that certain hydrogels exhibit LCST (lower critical solution temperature) at physiological temperatures, there is great potential for the use of these hydrogels in various biomedical applications such as cryopreservation of cells, drug delivery, and tissue engineering. Currently, researchers at the Ahmed Lab are studying the use of these hydrogels for cryopreservation of cells. Overall, the prospects of these hydrogels in biomedical research are promising.

6. References

1. Vitamin B5 (pantothenic acid). https://www.mountsinai.org/health-library/supplement/vitamin-b5-pantothenic-acid#:~:text=Vitamin%20B5%2C%20also%20called%20pantothenic,body%20use%20fats%20and%20protein (accessed Apr 5, 2023).

2.Kabir, A.; Dunlop, M. J.; Acharya, B.; Bissessur, R.; Ahmed, M. Water Recycling Efficacies of Extremely Hygroscopic, Antifouling Hydrogels. *RSC Advances* **2018**, *8* (66), 38100–38107.

3.Pantothenic acid. https://www.newworldencyclopedia.org/entry/Pantothenic_acid (accessed Apr 5, 2023).

4.Spry, C.; Chai, C. L.; Kirk, K.; Saliba, K. J. A Class of Pantothenic Acid Analogs Inhibits *Plasmodium Falciparum* Pantothenate Kinase and Represses the Proliferation of Malaria Parasites. *Antimicrobial Agents and Chemotherapy* **2005**, *49* (11), 4649–4657.

5.Preedy, V. R. *B vitamins and folate: Chemistry, analysis, function and effects*; RSC Publishing: Cambridge, 2013.

6.Combita, D.; Nazeer, N.; Bhayo, A. M.; Ahmed, M. Biomimetic and Hydrophilic Vitamin B5 Analogous Methacrylamide Polymers Prevent Surface Fouling. *ACS Applied Polymer Materials* **2022**, *4* (1), 575–585.

7.Basic polymer structure. https://www.e-education.psu.edu/matse81/node/2210 (accessed Apr 5, 2023).

8.Chen, J.; Garcia, E. S.; Zimmerman, S. C. Intramolecularly Cross-Linked Polymers: From Structure to Function with Applications as Artificial Antibodies and Artificial Enzymes. *Accounts of Chemical Research* **2020**, *53* (6), 1244–1256.

9.Pal, K.; Banthia, A. K.; Majumdar, D. K. Polymeric Hydrogels: Characterization and Biomedical Applications. *Designed Monomers and Polymers* **2009**, *12* (3), 197–220.

10.Shrivastava, A. Polymerization. *Introduction to Plastics Engineering* **2018**, 17–48.

11.Rane, S. S.; Choi, P. Polydispersity Index: How Accurately Does It Measure the Breadth of the Molecular Weight Distribution? *Chemistry of Materials* **2005**, *17* (4), 926–926.

12.Radke, W.; Held, D. Tips & Tricks GPC/Sec: Polydispersity - how broad is broad for macromolecules? https://www.chromatographyonline.com/view/tips-tricks-gpcsec-polydispersity-how-broad-broad-macromolecules-0 (accessed Apr 5, 2023).

13.Mishra, V.; Kumar, R. Living Radical Polymerization: A Review. Journal of Scientific Research. 2012, 56, 141-176

14.https://employees.csbsju.edu/cschaller/Advanced/Polymers/CPmw.html (accessed Apr 5, 2023).

15. Relationship between structure and function of molecules. https://knowledgeclass.blogspot.com/2013/08/relationship-between-structure-and.html (accessed Apr 5, 2023).

16.Raval, N.; Kalyane, D.; Maheshwari, R.; Tekade, R. K. Copolymers and Block Copolymers in Drug Delivery and Therapy. *Basic Fundamentals of Drug Delivery* **2019**, 173–201.

17.Crespy, D.; Rossi, R. M. Temperature-Responsive Polymers with LCST in the Physiological Range and Their Applications in Textiles. *Polymer International* **2007**, *56* (12), 1461–1468.

18. Chen, M. H.; Wang, L. L.; Chung, J. J.; Kim, Y.-H.; Atluri, P.; Burdick, J. A. Methods to Assess Shear-Thinning Hydrogels for Application as Injectable Biomaterials. *ACS Biomaterials Science & Engineering* **2017**, *3* (12), 3146–3160.

19. Clogston, J. D.; Patri, A. K. Zeta Potential Measurement. *Methods in Molecular Biology* **2010**, 63–70.

20. Nazeer, N.; Ahmed, M. Hydrophilic and salt responsive polymers promote depletion aggregation of bacteria. European Polymer Journal 2019, 119, 148-154.

21. Ahmed, E. M. Hydrogel: Preparation, Characterization, and Applications: A Review. *Journal of Advanced Research* **2015**, *6* (2), 105–121.

22. Bashir, S.; Hina, M.; Iqbal, J.; Rajpar, A. H.; Mujtaba, M. A.; Alghamdi, N. A.; Wageh, S.; Ramesh, K.; Ramesh, S. Fundamental Concepts of Hydrogels: Synthesis, Properties, and Their Applications. *Polymers* **2020**, *12* (11), 2702.

23. Z. Deng, H. Bouch´ekif, K. Babooram, A. Housni, N. Choytun and R. Narain, J. Polym. Sci., Part A: Polym. Chem., 2008, 46, 4984.

24.University, C. M. Natural vs synthetic polymers - gelfand center - carnegie Mellon University. https://www.cmu.edu/gelfand/lgc-educational-media/polymers/natural-synthetic-polymers/index.html#:~:text=Synthetic%20rubber%20is%20preferable%20because,design%20to%20give%20optimal%20properties. (accessed Apr 27, 2023).

25. Stevens, M. P. *Polymer chemistry: An introduction*; Oxford Univ. Pr.: Oxford, 1998.

26. DiRamio, J. A.; Kisaalita, W. S.; Majetich, G. F.; Shimkus, J. M. Poly(Ethylene Glycol) Methacrylate/Dimethacrylate Hydrogels for Controlled Release of Hydrophobic Drugs. *Biotechnology Progress* **2008**, *21* (4), 1281–1288.

27. Uman, S.; Dhand, A.; Burdick, J. A. Recent Advances in Shear-Thinning and Self-Healing Hydrogels for Biomedical Applications. *Journal of Applied Polymer Science* **2020**, *137* (25), 48668.

7. Appendices

Appendix A: NMR Spectra for B5AMA Synthesis (All NMR is taken by collogue Diego Combita)

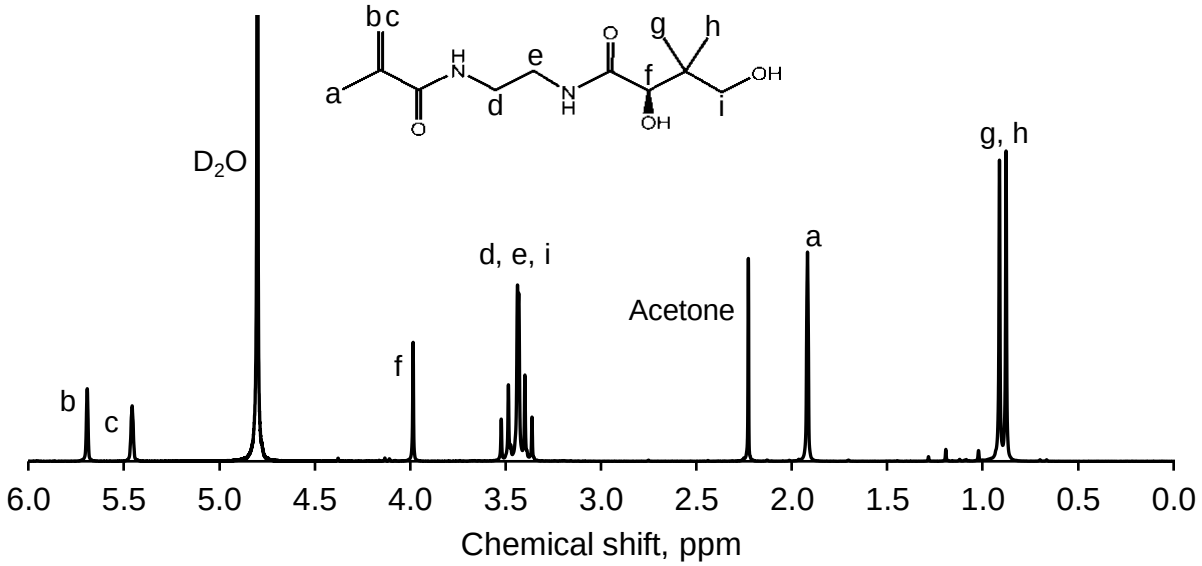

Figure 7.1:NMR spectrum for KW-5-1.

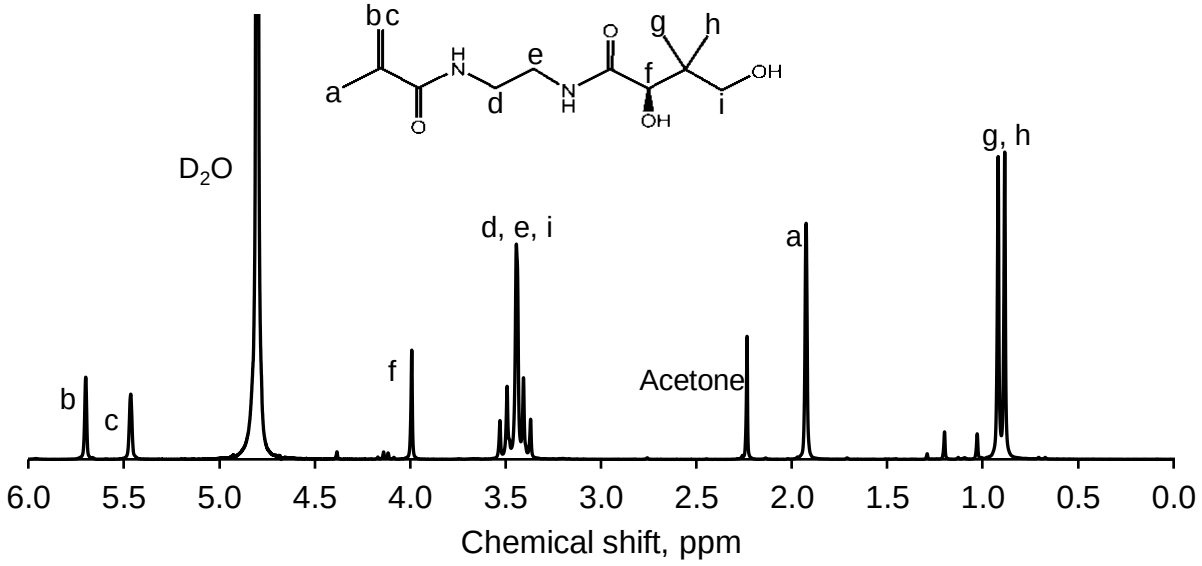

Figure 7.2: NMR spectrum for KW-11.

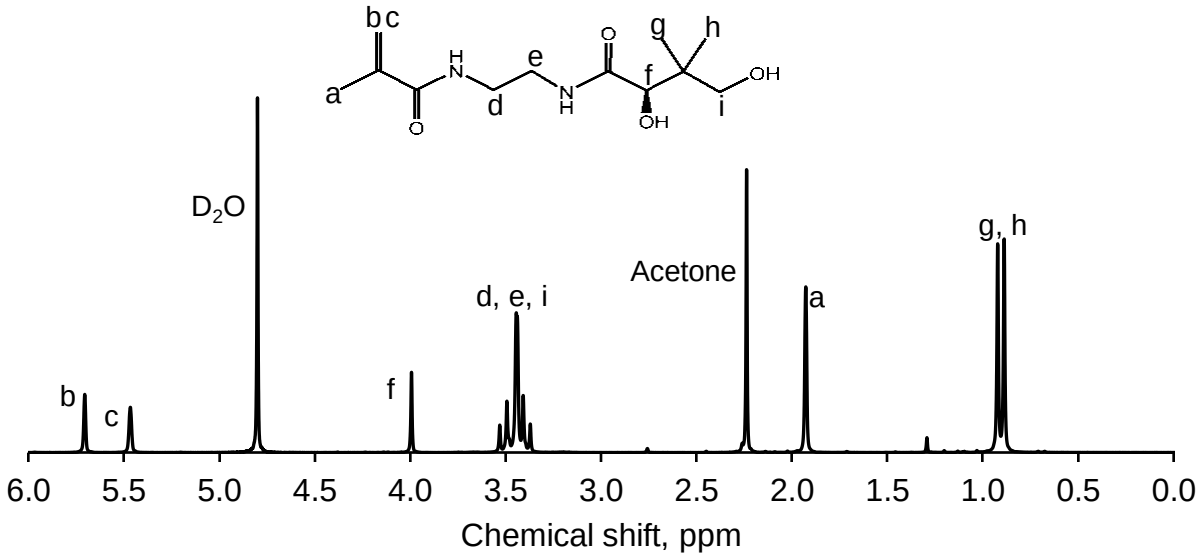

Figure 7.3: NMR spectrum for KW-26.

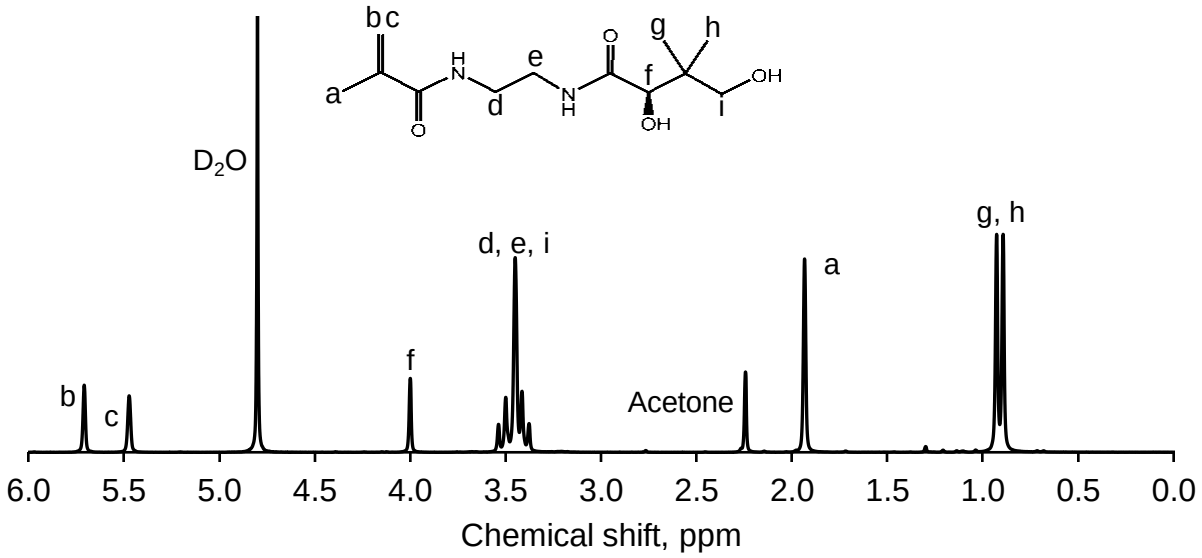

Figure 7.4:NMR spectrum for KW-32.

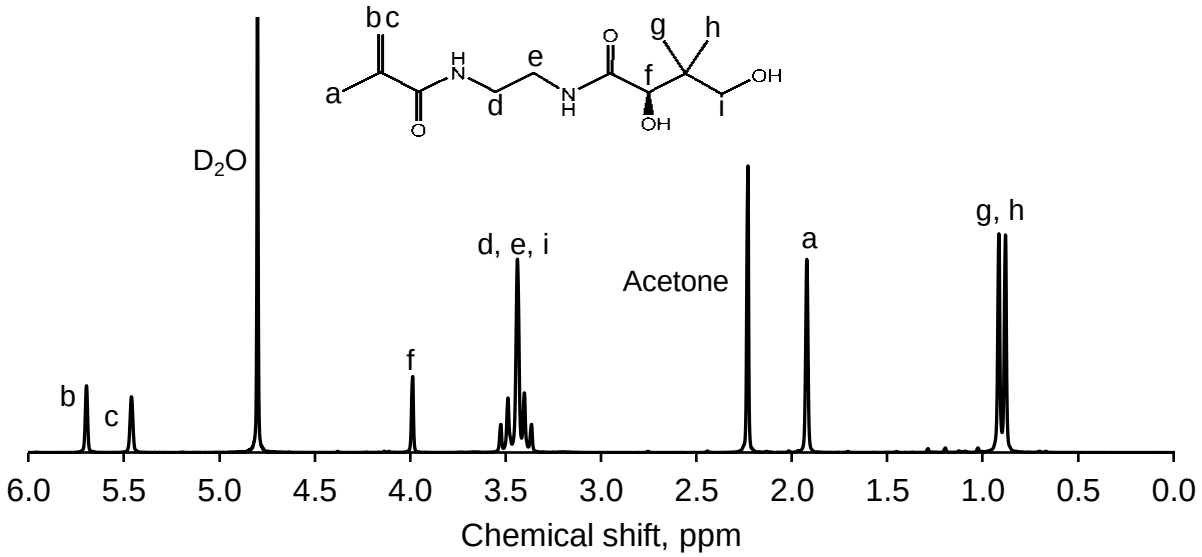

Figure 7.5: NMR spectrum for KW-33.

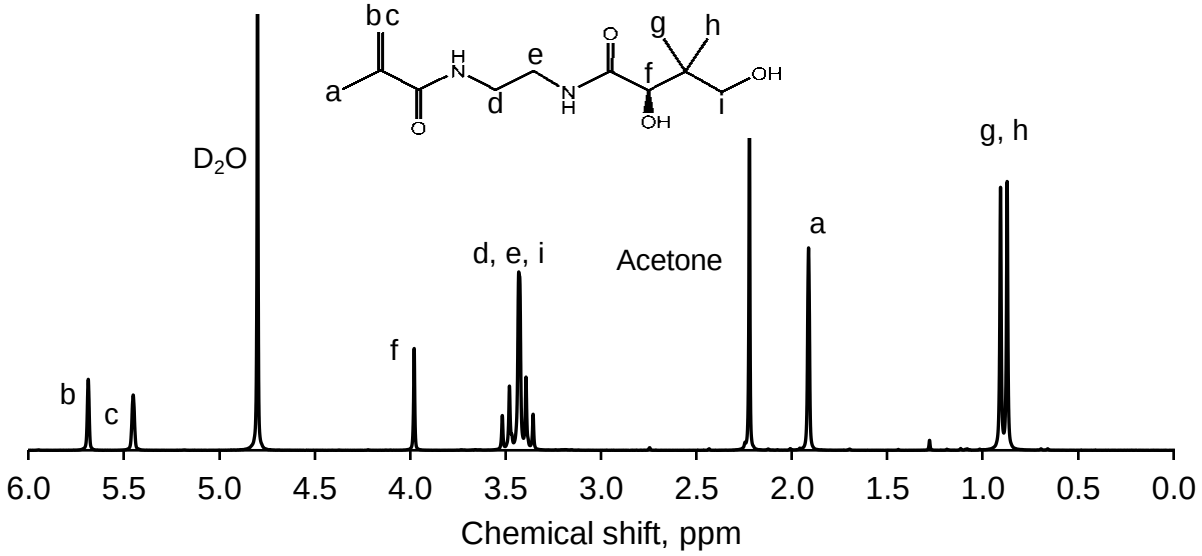

Figure 7.6: NMR spectrum for KW-36.

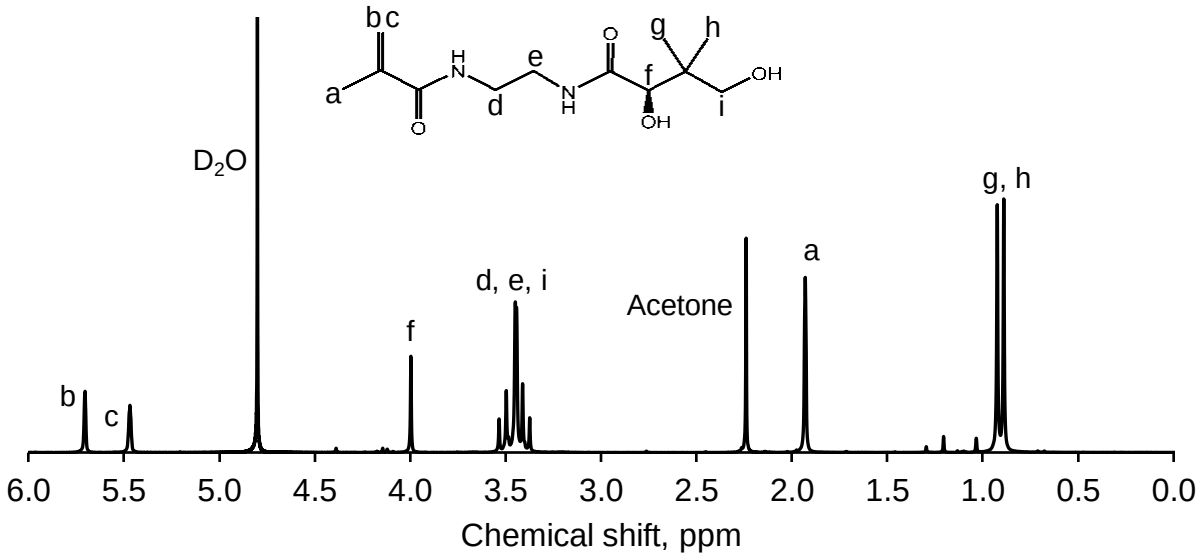

Figure 7.7:NMR spectrum for KW-40.

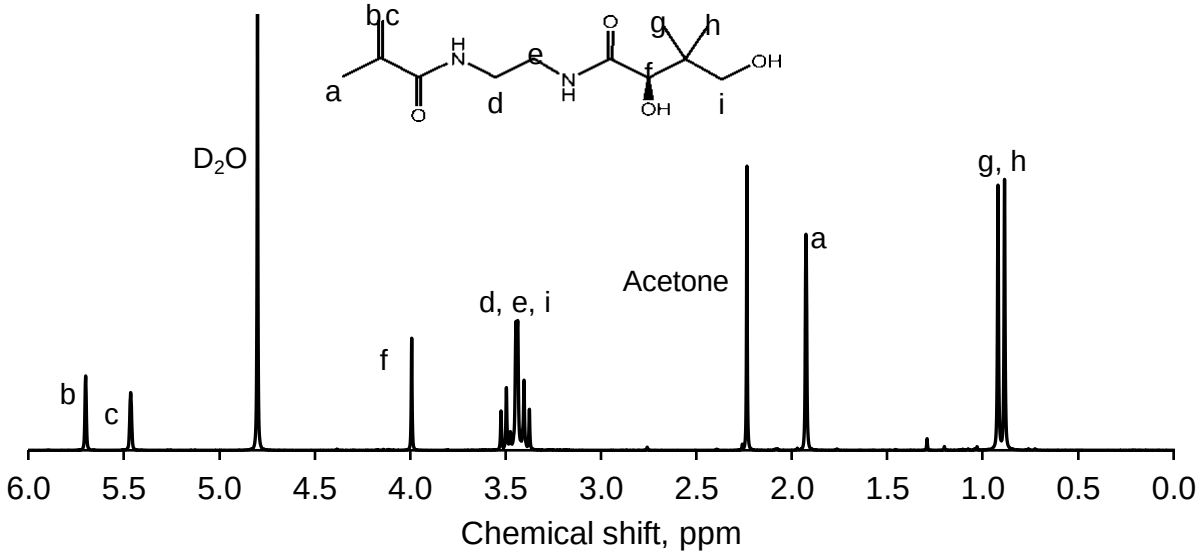

Figure 7.8: NMR spectrum for KW-43.

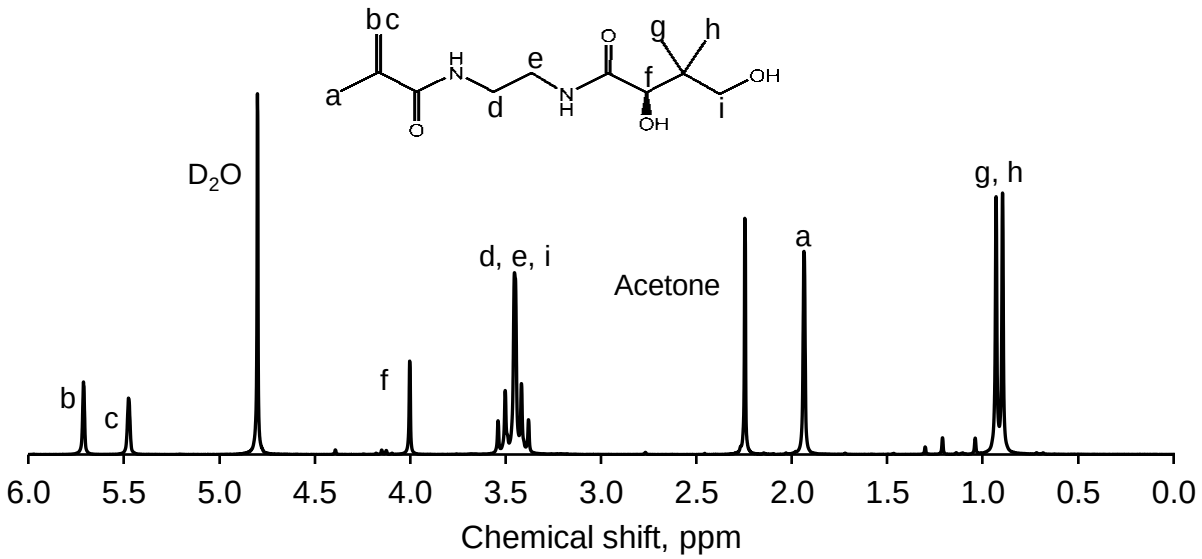

Figure 7.9: NMR spectrum for KW-45.

Appendix B: Data and Graphs for Swelling Kinetics

Table 7.1: Data for swelling kinetics study for KW-10-1.

KW-10-1 4% EGDMA					
Time (minutes)	Initial Weight (W_o) (g)	Weight after (W_t) (g)	Swelling Ratio	Swelling Ratio average	Time (Min)
15	0.0721	0.257	3.564	3.118	15
15	0.0832	0.2223	2.672		
30	0.0786	0.2769	3.523	2.995	30
30	0.0835	0.206	2.467		
60	0.0481	0.2231	4.638	3.752	60
60	0.0815	0.2336	2.866		
180	0.0566	0.3618	6.392	5.262	180
180	0.0839	0.3466	4.131		
300	0.0392	0.2647	6.753	5.941	300
300	0.0844	0.4329	5.129		

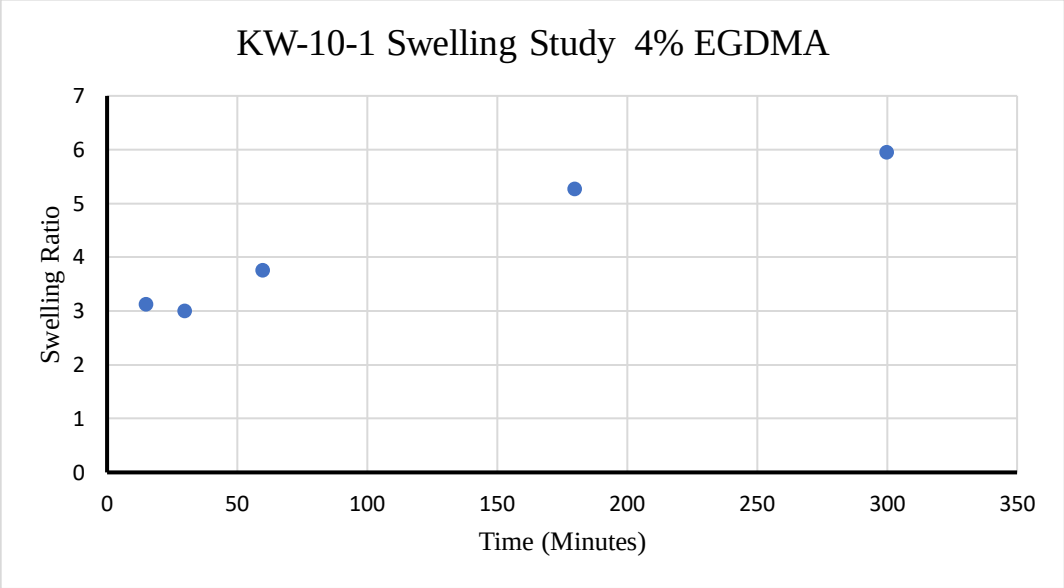

Figure 7.10: Swelling kinetics for KW-10-1.

Table 7.2: Data for swelling kinetics study for KW-10-2.

KW-10-2 7% EGDMA					
Time (Minutes)	Initial Weight (W_o) (g)	Weight after (W_t) (g)	Swelling Ratio (Wt/Wo)	Swelling Ratio average	Time (Min)
15	0.0734	0.3033	4.132	4.173	15
15	0.0747	0.3147	4.213		
30	0.0741	0.3352	4.524	4.052	30
30	0.0715	0.256	3.580		
60	0.0742	0.2089	2.815	3.263	60
60	0.0641	0.2379	3.711		
180	0.0708	0.3058	4.319	4.637	180
180	0.0738	0.3657	4.955		
300	0.0736	0.4535	6.162	6.400	300
300	0.0762	0.5051	6.629		

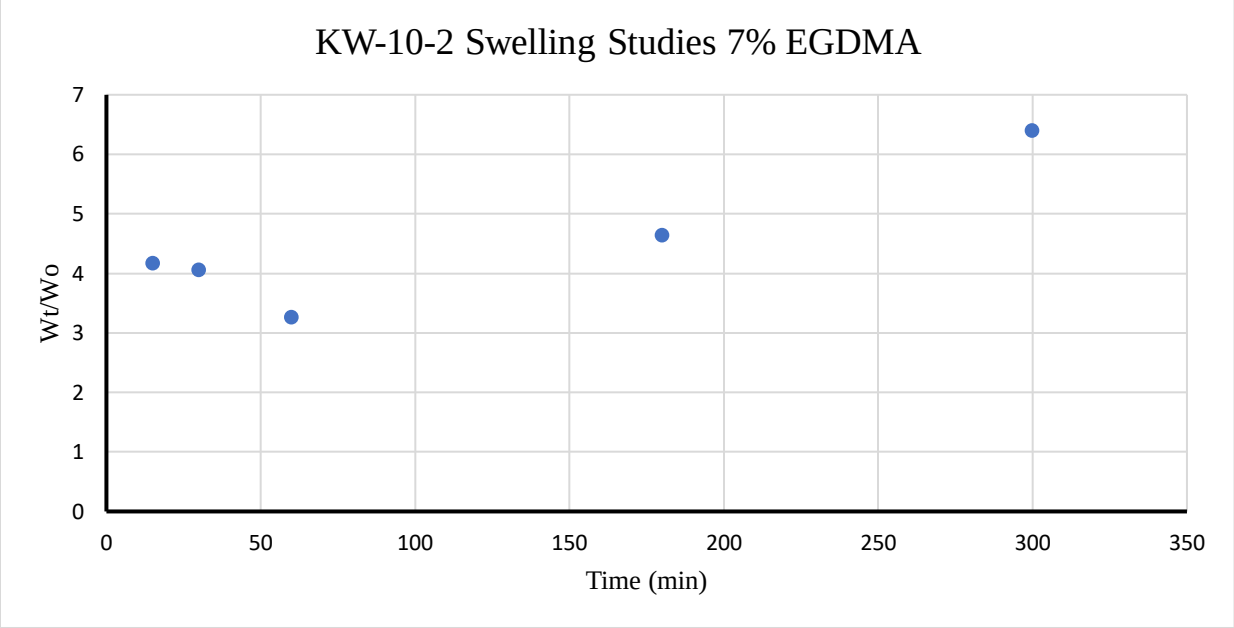

Figure 7.11: Graph for KW-10-2 Swelling Kinetics.

Table 7.3: Data for first swelling kinetics experiment with KW-13-1.

KW-13-1 7% EGDMA EXP1			
Time (Hours)	Initial Weight (W_o) (g)	Weight after (W_t) (g)	Swelling Ratio (Wt/Wo)
0.0833	0.0734	0.261	3.56
0.167	0.0731	0.286	3.92
0.250	0.0737	0.187	2.54
0.500	0.0726	0.308	4.24
1.00	0.0739	0.257	3.48
3.00	0.0758	0.551	7.26
5.00	0.0741	0.569	7.68
8.00	0.0735	0.589	8.01
24.0	0.0729	0.623	8.55

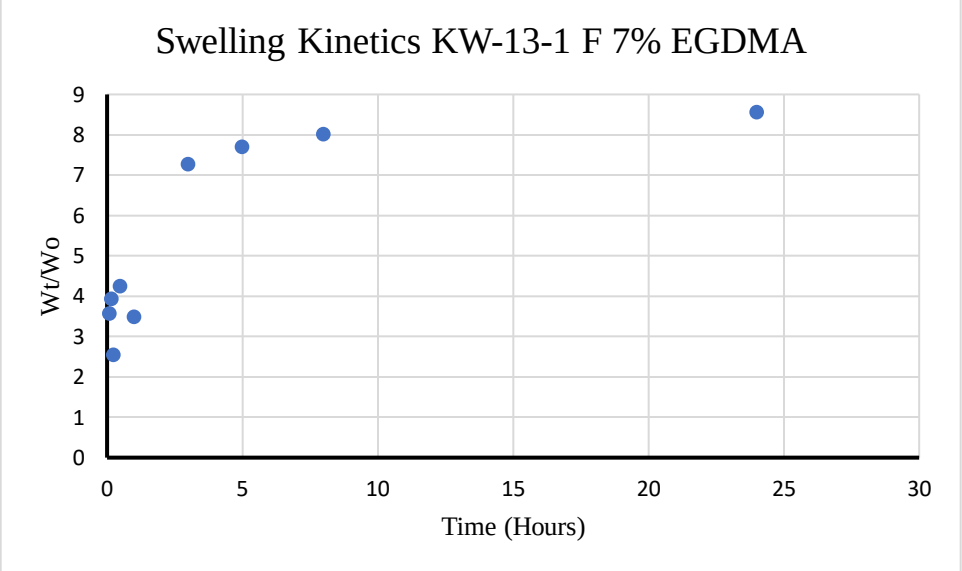

Figure 7.12: Graph showing swelling kinetics of KW-13-1 experiment 1.

Table 7.4: Data for second swelling kinetics experiment with KW-13-1.

KW-13-1 7% EGDMA EXP2			
Time (Hours)	Initial Weight (W_o) (g)	Weight after (W_t) (g)	Swelling Ratio (Wt/Wo)
0.0833	0.0758	0.203	2.68
0.167	0.0603	0.251	4.16
0.25	0.0748	0.213	2.85
0.50	0.0745	0.265	3.55
1.00	0.0751	0.333	4.44
3.00	0.0739	0.460	6.21
5.00	0.0697	0.561	8.04
8.00	0.0654	0.525	8.03
24.0	0.0728	0.629	8.64

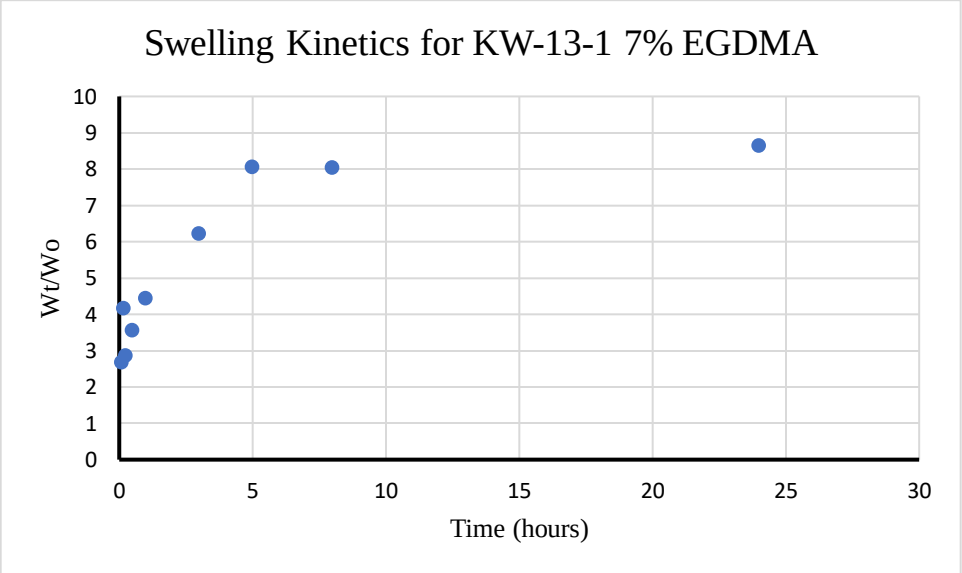

Figure 7.13: Graph showing swelling kinetics of KW-13-1 experiment 2.

Table 7.5: Data for third swelling kinetics experiment with KW-15-1.

KW-15-1 7% EGDMA EXP3			
Time (Hours)	Initial Weight (W_o) (g)	Weight after (W_t) (g)	Swelling Ratio (Wt/Wo)
0.0833	0.0810	0.233	2.89
0.167	0.0811	0.287	3.53
0.25	0.0735	0.271	3.69
0.50	0.0828	0.367	4.43
1.00	0.0823	0.435	5.29
3.00	0.084	0.451	5.37
5.00	0.082	0.569	6.94
8.00	0.0801	0.560	6.99
24.0	0.0817	0.503	6.16

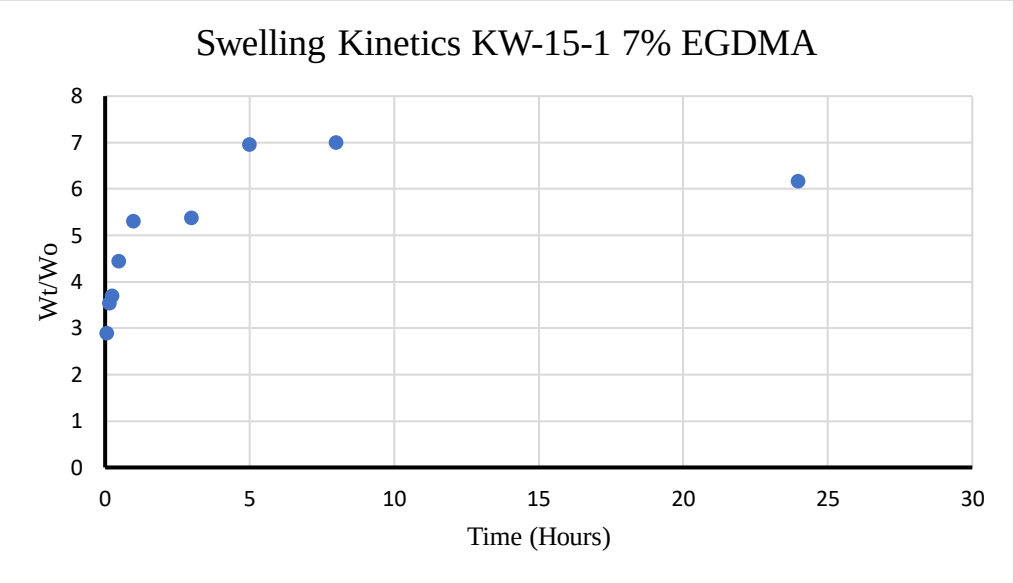

Figure 7.14: Graph showing swelling kinetics of KW-15-1 experiment 2.

Table 7.6: Data for average of swelling kinetic experiments 1,2 and 3.

Time (Hours)	KW-13-1 run 1 Swelling Ratios	KW-13-1 run 2 Swelling Ratios	KW-15-1 Swelling Ratios	Swelling Ratio (Average)	Standard Deviation
0.0833 (5 min)	3.56	2.68	2.89	3.04	0.460
0.167 (10 min)	3.92	4.16	3.53	3.87	0.310
0.250 (15 min)	2.54	2.85	3.69	3.03	0.590
0.500 (30 min)	4.24	3.55	4.43	4.07	0.460
1.00	3.48	4.44	5.29	4.40	0.900
3.00	7.26	6.21	5.37	6.28	0.950
5.00	7.68	8.04	6.94	7.56	0.560
8.00	8.01	8.03	6.99	7.68	0.590
24.0	8.55	8.64	6.16	7.78	1.41

Appendix C: Data and Graphs for Dynamic Light Scattering

Table 7.7: DLS data for KW-27-1.

Temperature (°C)	Run 1 Effective Diameter (nm)	Run 2 Effective Diameter (nm)	Run 3 Effective Diameter (nm)	Average Effective Diameter (nm)	Sample Standard Deviation
25	73.320	211.33	84.750	123.13	76.590
28	91.500	205.55	159.53	152.19	57.380
31	78.830	267.18	87.440	144.48	106.35
34	71.930	248.07	205.80	175.27	91.950
37	73.210	133.79	85.050	97.350	32.110
40	242.63	350.85	90.530	228.00	130.77
43	69.340	301.77	72.020	147.71	133.43
46	56.470	190.95	363.65	203.69	153.99
49	56.770	381.85	70.710	169.78	183.79
52	47.500	197.46	101.32	115.43	75.970
55	108.62	312.88	202.77	208.09	102.23
58	596.23	839.73	778.91	738.29	126.73
61	857.98	1206.0	1031.3	1031.8	174.00

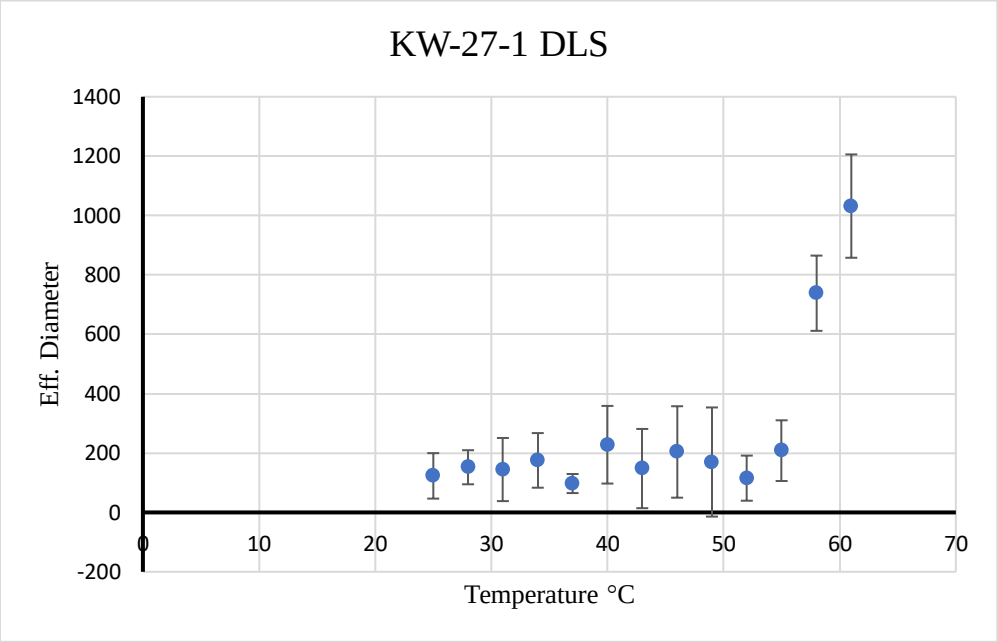

Figure 7.15: Graph of DLS data for KW-27-1 with error bars representing standard deviation.

Table 7.8: DLS data for KW-27-2.

Temperature (°C)	Run 1 Effective Diameter (nm)	Run 2 Effective Diameter (nm)	Run 3 Effective Diameter (nm)	Average Effective Diameter (nm)	Sample Standard Deviation
25	77.860	167.57	101.37	122.72	63.43
28	107.65	87.810	89.39	97.73	14.03
31	79.250	69.410	93.91	74.33	6.958
34	25.700	67.140	91.01	46.42	29.30
37	70.460	243.60	67.56	157.0	122.4
40	76.040	62.810	65.79	69.425	9.355
43	67.240	113.82	63.76	90.53	32.94
46	65.900	116.91	60.41	91.405	36.07
49	992.96	866.34	902.92	929.65	89.53
52	1496.7	1846.0	2251.23	1671.3	247.0
55	1896.4	2469.0	2684.36	2182.7	404.9
58	1965.9	2429.3	2662.6	2197.6	327.6
61	1560.9	2054.0	2555.93	1807.5	348.7

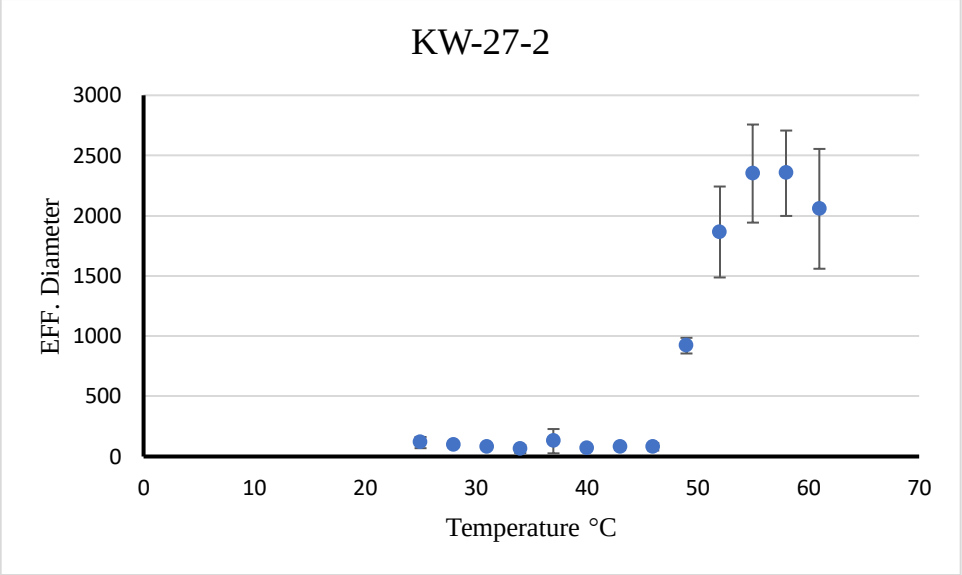

Figure 7.16: Graph of DLS data for KW-27-2 with error bars representing standard deviation.

Table 7.9: Data for DLS of KW-34-2.

Temperature (°C)	Run 1 Effective Diameter (nm)	Run 2 Effective Diameter (nm)	Run 3 Effective Diameter (nm)	Average Effective Diameter (nm)	Sample Standard Deviation
25	157.5	157.6	226.6	180.6	39.88
28	151.9	155.0	280.7	195.8	73.48
31	153.5	154.1	205.1	170.9	29.63
34	147.2	145.8	184.1	159.0	21.75
37	138.8	138.2	189.7	155.6	29.53
40	133.9	132.0	186.2	150.7	30.76
43	123.7	128.9	188.3	147.0	35.91
46	117.5	117.7	170.7	135.3	30.66
49	116.0	122.4	156.8	131.7	21.93
52	662.3	585.0	487.1	578.1	87.82
55	1368	2172	964.6	1502	614.6
58	1898	1625	4021	2515	1312
61	1412	1439	2292	1715	500.5

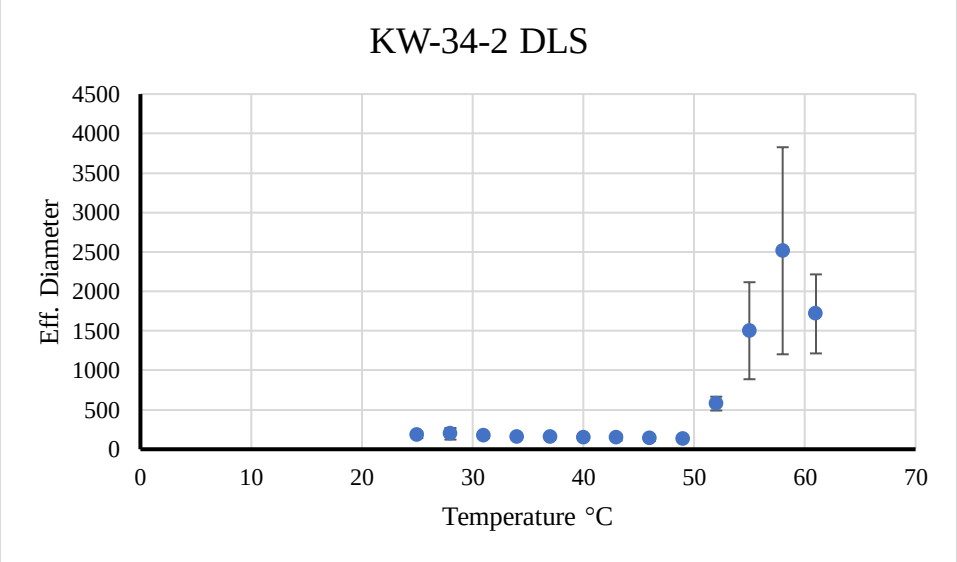

Figure 7.17: Graph of DLS data for KW-34-2 with error bars representing standard deviation.

Table 7.10: DLS data for DFC-722-2.

Temperature (°C)	Run 1 Effective Diameter (nm)	Run 2 Effective Diameter (nm)	Run 3 Effective Diameter (nm)	Average Effective Diameter (nm)	Sample Standard Deviation
25	82.33	232.2	157.7	157.2	74.91
28	65.37	72.59	80.93	68.98	7.787
31	86.03	71.35	82.17	78.69	7.610
34	67.06	68.91	72.48	67.99	2.755
37	69.14	70.68	101.5	69.91	18.26
40	64.32	76.40	68.63	70.36	6.122
43	57.51	203.1	56.06	130.3	84.50
46	95.59	65.61	54.69	80.60	21.18
49	949.1	522.8	493.5	736.0	255.0
52	833.0	1374	1974	1104	570.9
55	2266	2362	1903	2314	242.3
58	2080	2522	3774	2301	878.7
61	2150	1873	4387	2012	1378

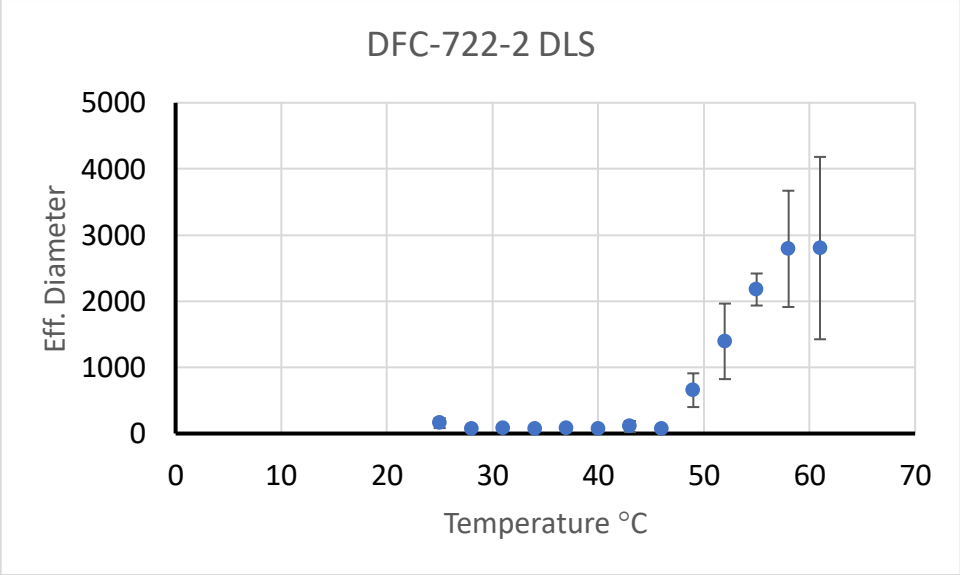

Figure 7.18: *Graph of DLS data for DFC-722-2 with error bars representing standard deviation.*

Table 7.11: DLS data for KW-7-1.

Temperature (°C)	Run 1 Effective Diameter (nm)
25	111.7
28	114.1
31	104.2
34	103.0
37	151.3
40	166.7
43	166.2
46	161.3
49	159.8
52	156.3
55	154.6
58	152.5
61	149.8

Table 7.12: *DLS data for KW-21-2.*

Temperature (°C)	Run 1 Effective Diameter (nm)
25	146.5
28	91.01
31	88.34
34	72.42
37	66.87
40	135.6
43	135.0
46	133.9
49	132.3
52	129.8
55	127.8
58	126.3
61	125.9

Table 7.13: DLS data for KW-21-1.

Temperature (°C)	Effective Diameter (nm)
25	62.38
28	55.89
31	53.73
34	50.27
37	202.5
40	222.4
43	216.6
46	215.1
49	210.0
52	205.2
55	202.2
58	196.4
61	192.2

Table 7.14: DLS data for KW-7-2.

Temperature (°C)	Effective Diameter (nm)
25	168.43
28	186.23
31	163.03
34	175.40
37	174.83
40	186.02
43	189.35
46	182.42
49	178.69
52	173.44
55	168.10
58	161.55
61	156.99

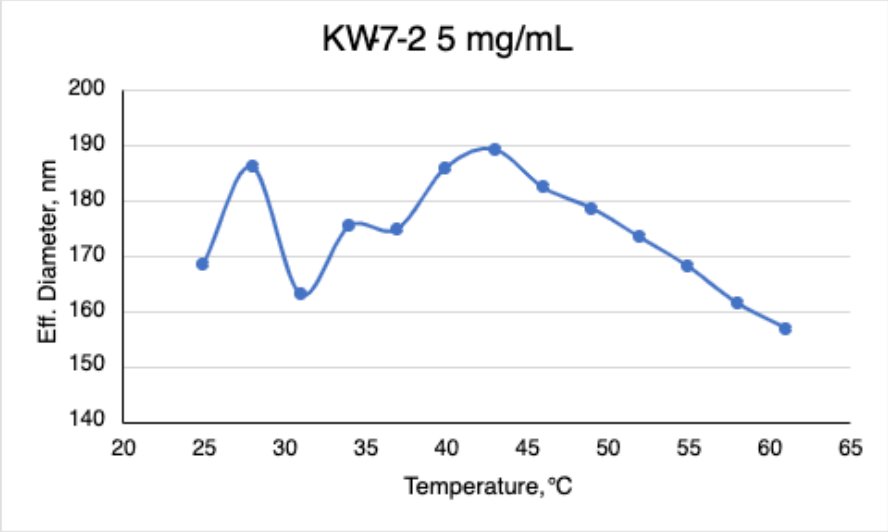

Figure 7.19: Graph of DLS data for KW-7-2.

Appendix D: Data for Absorbance Studies

Table 7.15: Absorbance data for KW-7.

Temperature (°C)	KW-7-1 Absorbance @625nm	KW-7-2 Absorbance @625nm
25	0.023688	0.070910
30	0.027304	0.051574
35	0.038449	0.098625
40	0.37030	0.82282
45	0.73788	0.96448
50	0.91322	1.1331
55	1.0020	1.1745
60	1.0065	1.1445

Table 7.16: Absorbance data for KW-21.

Temperature (°C)	KW-21-1 Absorbance @625nm	KW-21-2 Absorbance @625nm
22.5	0.0336	0.00172
30	0.0290	0.0180
35	0.0405	0.0251
40	0.239	0.105
45	0.596	0.320
50	0.801	0.433
55	0.729	0.528
60	0.944	0.540

Appendix E: Data and Graphs for Zeta-Potential

Table 7.17: Data for zeta-potential of KW-34-2.

	KW-34-2 Zeta-Potential		
Run	1	2	3
Zeta-Potential (mV)	3.54	2.32	4.06
Graph	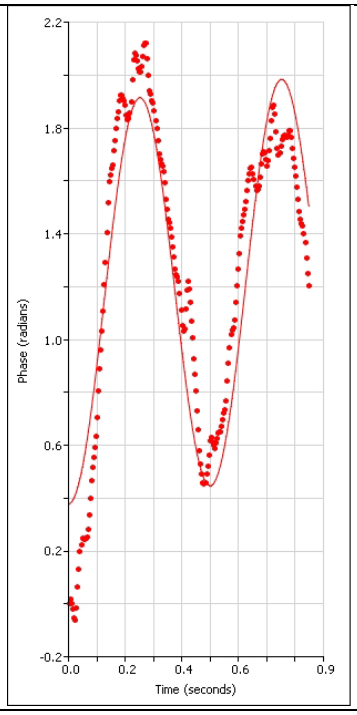	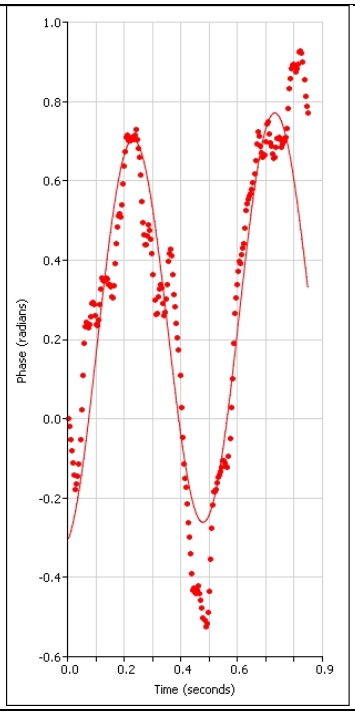	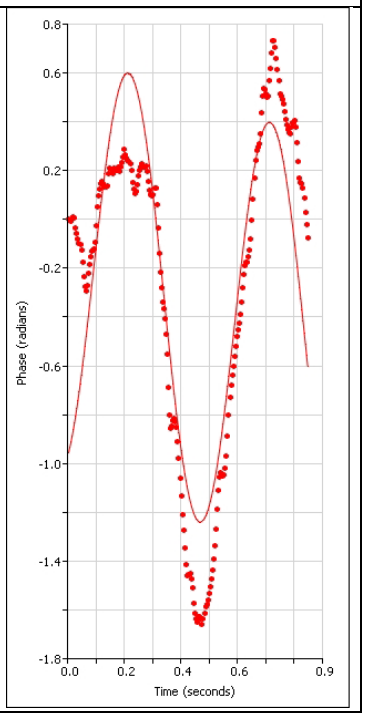

Table 7.18: Data for zeta-potential of KW-27-1.

	KW-27-1 Zeta-Potential		
Run	1	2	3
Zeta-Potential (mV)	-1.85	-0.72	-1.02
Graph	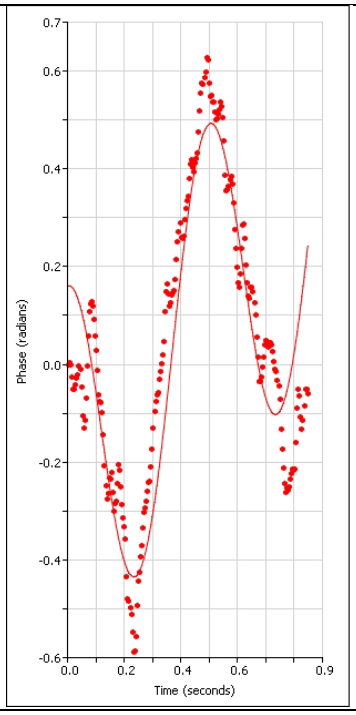	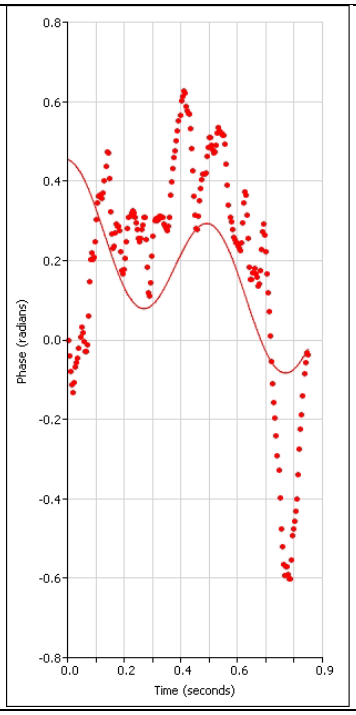	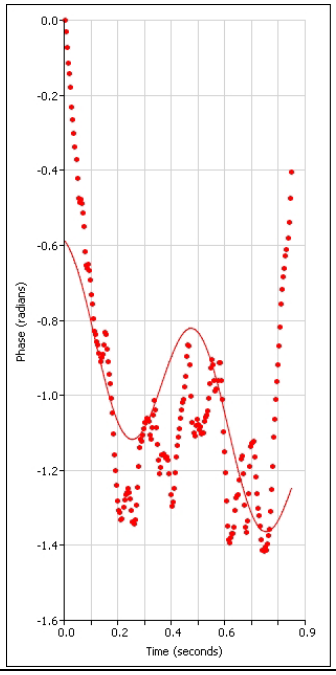

Table 7.19: Data for zeta-potential of KW-37-1.

	KW-37-1 Zeta-Potential		
Run	1	2	3
Zeta-Potential (mV)	1.34	0.69	0.93
Graph	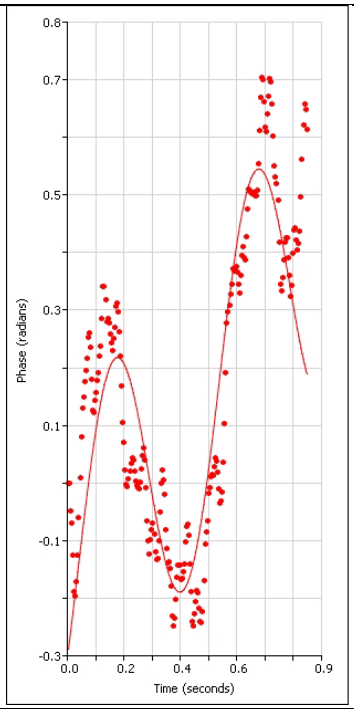	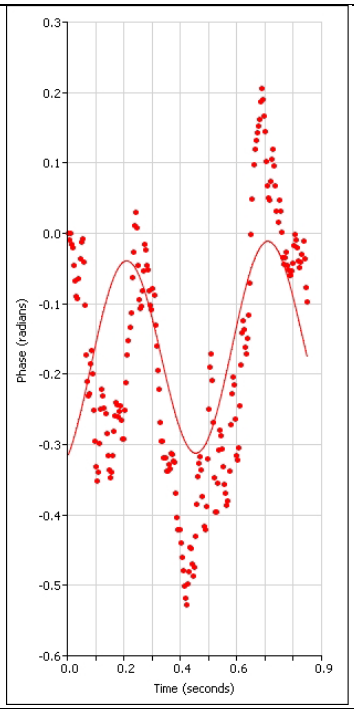	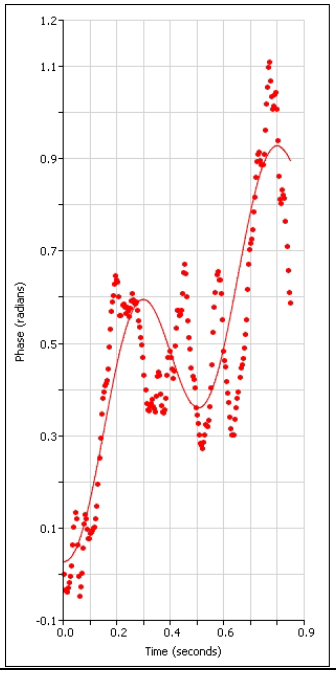

Table 7.20: Data for zeta-potential of DFC-722-2.

	DFC-722-2 Zeta-Potential		
Run	1	2	3
Zeta-Potential (mV)	-6.8	-6.78	-5.29
Graph	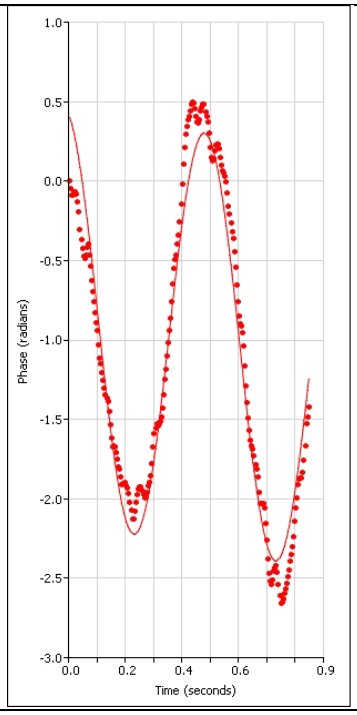	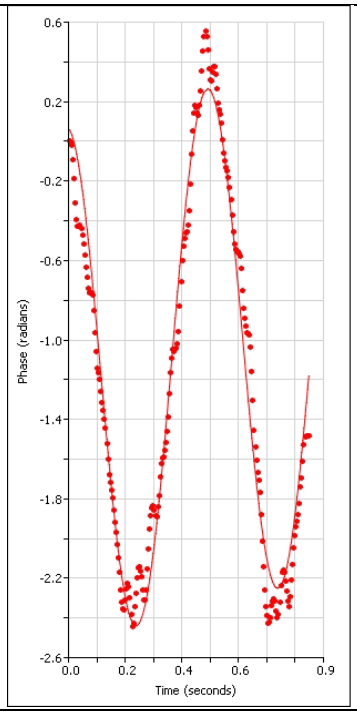	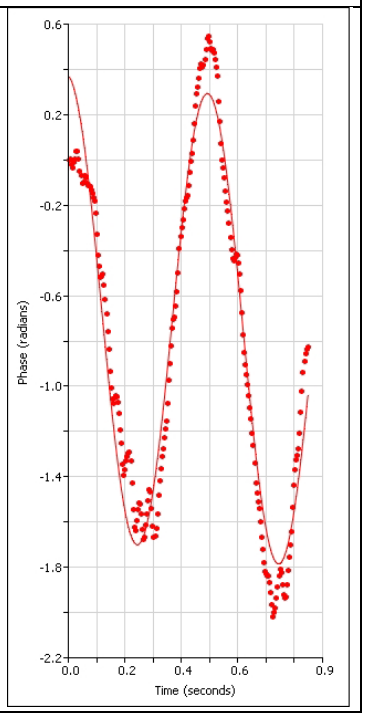

Table 7.21: Data for zeta-potential of KW-27-2.

	KW-27-2 Zeta-Potential		
Run	1	2	3
Zeta-Potential (mV)	-4.1	-4.32	-5.76
Graph